Thermochimica Acta 761 (2026) 180317

Contents lists available at ScienceDirect

Thermochimica Acta

journal homepage: www.elsevier.com/locate/tca

Experimental study and thermodynamic assessment of the reciprocal system Na^+, Ca^{2+} // Cl^-, SO_4^{2-}

Amedeo Morsa [a,*], Elena Yazhenskikh [a], Mirko Ziegner [a], Philipp Keuter [b], Michael Müller [a], Dmitry Sergeev [a,c]

[a] Forschungszentrum Jülich GmbH, Institute of Energy Materials and Devices, Structure and Function of Materials (IMD-1), D-52425, Jülich, Germany
[b] GTT-Technologies, Kaiserstraße 103, 52134 Herzogenrath, Germany
[c] NETZSCH-Gerätebau GmbH, D-52425, Selb, Germany

ARTICLE INFO

Keywords:
Phase change materials
Chlorides
Sulphates
Phase equilibria
Database development

ABSTRACT

This study aims to provide a comprehensive investigation of the reciprocal system Na^+, Ca^{2+}// Cl^-, SO_4^{2-} by integrating experimental analysis with thermodynamic modelling. The experimental approach involved the complementary use of Differential Thermal Analysis/Thermogravimetry (DTA/TG), Differential Scanning Calorimetry (DSC), and High-Temperature X-ray Diffraction (HT-XRD). These techniques provided essential experimental evidence for the phase equilibria description and served as a foundation for thermodynamic modelling. The reciprocal system was examined within the framework of phase change material (PCM) screening and identification for thermal energy storage applications. Based on the results obtained in this work, the thermodynamic database was developed for the aforementioned salt system. Notably, experimental findings highlighted significant modifications in the description of the binary system Na_2SO_4-$CaSO_4$, namely the formation of the solid solution based on the high temperature modification of Na_2SO_4 and the identification of intermediate compounds $Na_4Ca(SO_4)_3$, which replaces the previously assumed $Na_6Ca(SO_4)_4$ compound. Additionally, while $Na_2Ca(SO_4)_2$ had already been reported in prior studies, this work has provided a more precise definition of its thermal stability window, based on new experimental evidence. Furthermore, the experimental study of the NaCl-$CaSO_4$ and $CaCl_2$-Na_2SO_4 systems, representing the ionic exchange reaction, enabled a more detailed investigation of the reciprocal system, contributing to an improved thermodynamic description within the current database. This study reports, for the first time, the enthalpy of fusion of the eutectic composition in the NaCl-$CaSO_4$ system, determined to be 39.3 ± 1.7 kJ/mol, with a corresponding melting temperature of 724 °C (997 K). Through the thermodynamic assessment of the sub-systems investigated both in this study and in previous works, an updated thermodynamic database has been developed, providing a comprehensive description of the entire reciprocal system and enabling a more accurate estimation of eutectic compositions within it. These findings enhance the accuracy of phase equilibria modelling and provide valuable insights into the thermal properties of potential PCM candidates.

1. Introduction

The thermodynamic study of sodium and calcium chlorides and sulphates is essential for various industrial and environmental applications. In particular, these salts play a key role in desulphurisation processes, where they enhance limestone dissolution, improve SO_2 capture efficiency, and optimise pH stability in wet Flue Gas Desulphurisation (FGD) systems [1]. Additionally, they are relevant in industrial waste treatment and metallurgical purification processes [2], water treatment [3], and polymer composites and cement manufacturing [4], where their thermodynamic behaviour influences reactivity, phase stability, and overall system performance. Beyond these applications, inorganic sodium and calcium salts have significant potential as Phase Change Materials (PCMs) for Thermal Energy Storage (TES) [5]. Whether used alone or in combination, they exhibit properties that align with the requirements of effective PCMs, such as high latent heat, thermal stability, and cost-effectiveness [6,7]. To identify optimal candidates, including intermediate compounds or eutectic mixtures based on these salts, a

* Corresponding author.
E-mail address: amedeo.morsa@julumni.fz-juelich.de (A. Morsa).

https://doi.org/10.1016/j.tca.2026.180317
Received 19 January 2026; Received in revised form 15 April 2026; Accepted 19 April 2026
Available online 23 April 2026

Table 1
Sample Table.

Chemical Name	CAS number	Source	Initial Purity (supplier specification)	Pre-treatment	Analysis method
NaCl	7647–14–5	Thermo Fisher Scientific	anhydrous 99.998%)	Dried at 150 °C under vacuum for 24 h	XRD; DTA/TG
$CaCl_2$	10,043-52–4	Alfa Aesar	anhydrous 99.99%	Dried at 150 °C under vacuum for 24 h	XRD; DTA/TG
Na_2SO_4	7757–82–6	Thermo Fisher Scientific	anhydrous 99.9955%	Dried at 150 °C under vacuum for 24 h	XRD; DTA/TG
$CaSO_4$	7778–18–9	Alfa Aesar	anhydrous 99.993%	Dried at 150 °C under vacuum for 24 h	XRD; DTA/TG

comprehensive thermodynamic study is necessary. Developing a reliable thermodynamic database enables the accurate prediction of phase equilibria, thermal properties, and melting behaviours, which are crucial for both fundamental research and practical implementation in TES systems and beyond.

The Na^+, Ca^{2+} // Cl^-, SO_4^{2-} was previously studied experimentally by Palkin [8], Zimina et al. [9], and Rowe et al. [10]. The system consists of four binary systems NaCl-$CaCl_2$, Na_2SO_4-$CaSO_4$, NaCl-Na_2SO_4 and $CaCl_2$-$CaSO_4$ as edges and two sections representing the exchange reaction Na_2Cl_2-$CaSO_4$ and $CaCl_2$-Na_2SO_4 as diagonals, where NaCl is considered as a dimer (Na_2Cl_2) to maintain electroneutrality. Zimina et al. [9] reported no ternary compounds, a eutectic point at 485 °C in the pseudo-ternary system Na_2Cl_2-$CaCl_2$-$CaSO_4$ and sulphate solid solution in the Na_2Cl_2-Na_2SO_4-$CaSO_4$.

The literature reports conflicting data on phase equilibria in several binary sub-systems. For instance, the existence of the double sulphates 3:1 in the system Na_2SO_4-$CaSO_4$ [11] is inconsistent with reports of solid solubility based on Na_2SO_4 [12,13]. In order to develop a reliable thermodynamic dataset, the phase equilibria and thermodynamic properties need to be experimentally verified. Therefore, a comprehensive experimental investigation was conducted, employing various characterisation techniques, with the aim of clarifying phase relationships and supporting future thermodynamic modelling.

The thermodynamic descriptions available in the literature for the binary sub-systems employ different models for the liquid phase - e.g. NaCl-$CaCl_2$ [14–16], Na_2SO_4-$CaSO_4$ [17–19], NaCl-Na_2SO_4 [20,21], $CaCl_2$-$CaSO_4$ [22] - which makes it impossible to derive a consistent dataset for the complete reciprocal system. In the present study, the thermodynamic database of the system Na^+, Ca^{2+} // Cl^-, SO_4^{2-} is generated in the framework of the study on the complex salt system Na^+, K^+, Mg^{2+}, Ca^{2+} // Cl^-, SO_4^{2-} [23] for interpolative and predictive thermodynamic calculations. The present experimental results on phase equilibria and thermodynamic properties are included into the thermodynamic modelling along with the selected literature data. The Gibbs energy parameters of the solid and liquid phases are adjusted in accordance with all available experimental data. The modified associate species model proposed by Besmann et al. [24] is adopted, given the successful application to many oxide [25] and salt systems [19,26–28], considering the sulphates and chlorides as "binary species" to keep consistence with our general database [29].

2. Experimental

2.1. Samples

The pure compounds NaCl (CAS 7647-14-5, Thermo Fisher Scientific, anhydrous 99.998%), $CaCl_2$ (CAS 10,043-52-4, Alfa Aesar, anhydrous 99.99%), Na_2SO_4 (CAS 7757-82-6, Thermo Fisher Scientific, anhydrous 99.9955%) and $CaSO_4$ (CAS 7778-18-9, Alfa Aesar, anhydrous 99.993%) were used as starting materials for preparing the studied mixtures (Table 1). Prior to use, the powders were dried in a vacuum furnace at 150 °C for 24 h to eliminate any residual moisture. All sample handling was performed in a glove box ($O_2 < 0.5$ ppm, $H_2O < 1$ ppm) under a dry argon atmosphere to prevent contamination. The mixtures were directly prepared into crucibles according to the stoichiometric ratio, with sampling amounts ranging from 50 to 100 mg. The determination of the melting temperature of the pure compounds and mixtures under study proved challenging due to the decomposition of the sulphates into oxides before reaching their melting temperatures [17,30–33]. To mitigate this issue and minimise mass loss, sealed platinum tubes were used to conduct the measurements at high temperatures, as previously adopted in earlier studies [22,26].

2.2. Instruments

2.2.1. Differential thermal analysis and thermal gravimetry (DTA/TG)

A STA 449C Jupiter (Netzsch), equipped with a silicon carbide oven (RT-1600 °C) and a perpendicular sample holder with type S thermocouple (Pt/(Pt10Rh)), was used for DTA measurements in the present study. The temperature calibration was performed using the characteristic phase transition temperatures of a set of reference compounds, namely C_6H_5COOH (122.5 °C), $RbNO_3$ (164.2 °C), $KClO_4$ (300.8 °C), Ag_2SO_4 (462.2 °C), CsCl (470.0 °C), K_2CrO_4 (668.0 °C), $BaCO_3$ (808.0 °C), K_2SO_4 (1069.0 °C), and CaF_2 (1418.0 °C). All calibration measurements were conducted using sealed platinum tubes placed in alumina DTA crucibles. The average temperature deviation was ±5 °C, corresponding to a standard uncertainty of u(T) = 3 °C. An inert argon atmosphere was maintained during the experiments with a constant gas flow of 20 ml/min. The thermal protocol consisted of three consecutive heating and cooling cycles at a rate of 5 K/min. Data evaluation was performed using the Netzsch Proteus Analysis software. Consistent thermal behaviour was observed from the second heating-cooling cycle onward. For the purposes of the present analysis, phase transition temperatures were extracted mainly from the heating curves. Eutectic temperatures were determined from the onset of the corresponding thermal effect, whereas the peak maxima associated with subsequent transitions were assigned to either liquidus temperatures or solid-solid phase transformations. However, certain thermal events were only evident during the cooling cycle; in such cases, the temperatures were determined from the cooling curves, while the general approach remained based on the heating cycle. To mitigate mass loss caused by decomposition of sulphates and vaporisation of chlorides, sealed platinum crucibles were used for analysis. The crucible was closed by folding the upper end after filling the sample (50–100 mg) under dry argon in a glove box and then welded outside the glove box with a hydrogen/oxygen flame.

2.2.2. Differential scanning calorimetry (DSC)

Heat-capacity measurements on the selected compositions were carried out with a Calvet-type DSC instrument (mHTC 96, Setaram). Two different experimental procedures were adopted in order to account for the distinct measurement conditions. Low-temperature experiments were conducted in an open system, where no mass loss was expected. This approach was specifically used for calorimetric measurements of eutectic mixtures, where the melting temperature remained within a range that prevented mass loss - neither due to the vapor pressure of chlorides nor to sulphate decomposition. Conversely,

Table 2
Thermodynamic data of stochiometric compounds used in the present work.

Compound	$\Delta H^0_{298,f}$ J/mol	S^0_{298} J/mol•K	T K	C_p J/mol•K	Ref.
NaCl	−411,120 [42]	72.132 [42]	1–20	$0.08112742793394T - 0.010415905513837^2 + 0.000524656971697^3$	[16]
			20–116	$-10.6712089631739 + 0.6130440076047T - 5.0146910679•10^{-4}T^2 - 9.09935974•10^{-6}T^3$	[16]
			116–298	$12.937383161886 + 0.33737791631461T - 1.08663138387•10^{-3}T^2 + 1.26668694•10^{-6}T^3$	[16]
			298–900	$56.304 - 0.0130328T - 342570T^{-2} - 2.18749998•10^{-5}T^2$	[36]
			900–1076	$59.853 - 0.0194622T - 688110T^{-2} - 2.51622•10^{-5}T^2$	[36]
NaCl (liquid)	−391,305 [16]	82.493 [16]	S→L ΔH_{tr} = 28.2 kJ/mol at 1076 K (803 °C)		[42]
			1–20	$0.08112742793394T - 0.010415905513837^2 + 0.000524656971697^3$	[16]
			20–116	$-10.6712089631739 + 0.6130440076047T - 5.0146910679•10^{-4}T^2 - 9.09935974•10^{-6}T^3$	[16]
			116–178	$12.937383161886 + 0.33737791631461T - 1.08663138387•10^{-3}T^2 + 1.26668694•10^{-6}T^3$	[16]
			178–3000	68.45	[16]
$CaCl_2$	−795,797 [36]	104.602 [36]	1–50	$0.781554231489 - 0.123592918725T + 0.0306270315625T^2 - 0.000349282014374T^3$	[16]
			50–180	$-16.7324902861 + 1.16864188717T - 0.00602988655099T^2 + 1.16627589852•10^{-5}T^3$	[16]
			180–600	$43.9252039771 + 0.171967748287T - 0.000310281876053T^2 + 1.97728034832•10^{-7}T^3$	[16]
			600–1045	$77.9360892352 - 0.00630254569051T + 6.57695847866•10^{-6}T^2 + 7.52474112684•10^{-9}T^3$	[16]
			1045–3000	87.12	[16]
$CaCl_2$ (liquid)	−786,861 [16]	104.602 [16]	S→L ΔH_{tr} = 28.5 kJ/mol at 1045 K (772 °C)		[36]
			1–50	$0.781554231489 - 0.123592918725T + 0.0306270315625T^2 - 0.000349282014374T^3$	[16]
			50–180	$-16.7324902861 + 1.16864188717T - 0.00602988655099T^2 + 1.16627589852•10^{-5}T^3$	[16]
			180–486	$43.9252039771 + 0.171967748287T - 0.000310281876053T^2 + 1.97728034832•10^{-7}T^3$	[16]
			486–3000	116	[16]
Na_2SO_4 (LT)	−1387,900 [36]	149.58 [36]	1–34	$2.86•10^{-4}T^3$	[19]
			34–298	$60.363842 + 0.3702618T + 37,895.87535T^{-2} - 3.6413037•10^{-4}T^2 - 3197.4504/T$	[19]
			298–458	$80.81543 + 0.1586519T$	[36]
			458–514	$93.34096 + 0.1313035T$	[36]
			514–1157	$161.54872 + 0.01536T - 4636,382.93347T^{-2} + 3.31857•10^{-5}T^2$	[19]
			1157–3500	197.033	[36, 19]
Na_2SO_4 (MT)	−1387,600 [36]	150.235 [36]	LT→MT ΔH_{tr} = 0.3 kJ/mol at 458 K (185 °C), C_p like Na_2SO_4 (LT)		[36]
Na_2SO_4 (HT)	−1378,105 [19]	168.233 [19]	MT→HT ΔH_{tr} = 10.9 kJ/mol at 514 K (241 °C)		[36]
			1–34	$2.86•10^{-4}T^3$	[19]
			34–298	$60.363842 + 0.3702618T + 37,895.87535T^{-2} - 3.6413037•10^{-4}T^2 - 3197.4504/T$	[19]
			298–514	$62.99363 + 0.21808T$	[19]
			514–1157	$208.1015 - 0.1314436T + 1485.492T^{-2} + 1.323406•10^{-4}T^2$	[36]
			1157–3500	197.033	[36, 19]
Na_2SO_4 (liquid)	−1365,585 [19]	158.177 [19]	HT→L ΔH_{tr} = 23.5 kJ/mol at 1157 K (884 °C)		[36]
			1–34	$2.86•10^{-4}T^3$	[19]
			34–265	$60.363842 + 0.3702618T + 37,895.87535T^{-2} - 3.6413037•10^{-4}T^2 - 3197.4504/T$	[19]
			265–3500	197.033	[36, 19]
$CaSO_4$ (LT)	−1437,622 [36]	107.492 [43]	1–39	$1.58639676•10^{-4}T^3$	[19]
			39–298	$60.2427676 + 0.22021804T + 73,416.5259T^{-2} - 1.3048247•10^{-4}T^2 - 4185.07635/T$	[19]
			298–1784	$100.854288 + 0.06896988T - 1736,052.08T^{-2} - 8.6603105•10^{-6}T^2$	[19]
			1784–2000	195.63	[26]
$CaSO_4$ (HT)	−1420,012 [19]	119.282 [19]	LT→HT ΔH_{tr} = 17.6 kJ/mol at 1493.6 K (1220.4 °C), C_p like $CaSO_4$ (LT)		[19, 26]
$CaSO_4$ (liquid)	−1425,938 [19]	107.714 [26]	HT→L ΔH_m = 16 kJ/mol at 1783.6 K (1510.4 °C)		[19, 26]
			1–39	$1.58639676•10^{-4}T^3$	[19]
			39–298	$60.2427676 + 0.22021804T + 73,416.5259T^{-2} - 1.3048247•10^{-4}T^2 - 4185.07635/T$	[19]
			298–795	$100.854288 + 0.06896988T - 1736,052.08T^{-2} - 8.6603105•10^{-6}T^2$	[19]
			795–2000	195.63	[19]
$Na_2Ca(SO_4)_2$	−2805,571 [a]	296.5011 [a]	1–40	$0.0404823106512207T - 0.011386782654179T^2 + 0.00119850154098668T^3 - 3.47493555383553•10^{-5}T^4 + 5.66348660882418•10^{-7}T^5 - 3.50955711217862•10^{-9}T^6$	[19], [a]
			40–298	$485.770729051669 - 3.16102420452602T + 520,131.074911487T^{-2} + 0.0250441741230522T^2 - 8.70656764614227•10^{-5}T^3 + 1.08439154194594•10^{-7}T^4 - 28,176.9046664479T^{-1}$	[a]
			298–1183	$199.01893 + 0.22177562T - 2559,395.63T^{-2} - 6.90796848•10^{-5}T^2$	[a]
$Na_4Ca(SO_4)_3$	−4216,029 [a]	406.652 [a]	34–39	$120.727684 + 0.7405236T + 75,791.7507T^{-2} + 0.00072826074T^2 - 0.000158639676T^3 - 6394.9008T^{-1}$	[a]
			39–298	$180.9704516 + 0.96074164T + 149,208.2766T^{-2} - 0.00085874321T^2 - 10,579.97715T^{-1}$	[a]
			298–458	$262.485148 + 0.386273682T - 1736,052.08T^{-2} - 8.6603105•10^{-5}T^2$	[a]
			458–514	$287.536208 + 0.331576882T - 1736,052.08T^{-2} - 8.6603105•10^{-5}T^2$	[a]
			514–1157	$423.951728 + 0.099689882T - 11,008,817.94694T^{-2} + 5.77110895•10^{-5}T^2$	[a]
			1157–1780	$494.920288 + 0.068969882T - 1736,052.08T^{-2} - 8.6603105•10^{-5}T^2$	[a]
			1780–3500	589.699423117135	[a]

[a] this work.

high-temperature measurements were carried out for sulphate-based mixtures, where temperatures exceeding 1000 °C were reached. In such cases, an open system would have resulted in significant mass loss, making sealed crucibles necessary. For the low-temperature experiments, 200–300 mg of powdered sample was placed in an alumina liner within a platinum crucible and a platinum lid. For the high-temperature measurements, a 50–100 mg sample was loaded into a sealed platinum tube, positioned in a platinum sample holder, ensuring accurate analysis without mass loss. All DSC measurements were performed at a constant heating rate of 4 K/min under He with a flow of 5 ml/min. Different calibration standards were adopted depending on the measurement protocol. In the first case, temperature and enthalpy calibrations relied on pure metals: In (156.6 °C), Sn (231.9 °C), Pb (327.5 °C), Zn (419.5 °C), Al (660.3 °C), and Ag (961.8 °C). In the second case, selected pure salts were used: $BaCO_3$ (808.0 °C), Na_2SO_4 (241 °C and 884 °C), K_2SO_4 (584 °C and 1069 °C), and MgF_2 (1263 °C). The determination of the heat capacity (C_p°, J•mol^{-1}•K^{-1}) was carried out according to the three-step ratio method [34], using sapphire (α-Al_2O_3, NIST Standard Reference Material SRM720, purity 99.95%, metal basis) [35] as a reference, and is expressed by the following equation:

$$C^{\circ}_{p(s)} = \frac{m_r}{m_s}\cdot\frac{DSC_s - DSC_b}{DSC_r - DSC_b}\cdot C^{\circ}_{p(r)} \quad (1)$$

where m is the mass of the substance (g), DSC is the signal of thermopile (μV), and subscripts b, r and s stand for baseline, reference and sample respectively. For each sample, independent baseline and reference runs were conducted. The choice of sapphire reference depended on the experimental setup: stacked sapphire discs were used when a platinum crucible with an alumina liner was employed, whereas small sapphire cylinders (~1 mm in diameter) served as the reference when platinum tubes were used as crucibles.

2.2.3. High temperature X-ray diffractometry (HT-XRD)

High-temperature X-ray diffraction (HT-XRD) measurements in the present work were carried out using an Empyrean diffractometer from Malvern PANalytical configured with a Cu-LFF X-ray tube (operated at 40 kV and 40 mA), BBHD mirror, and a PIX-cel3D detector. An Anton Paar HTK 1200 N high-temperature chamber was employed to enable in situ heating, while a continuous flow of synthetic air was maintained throughout the experiments. Lattice parameters and the relative amounts of secondary phases were determined through Rietveld refinement using the profile analysis software TOPAS (version 6, Bruker AXS). Crystallographic information required for the refinements was taken from the Inorganic Crystal Structure Database (ICSD). The uncertainty for temperature was estimated to be ±5 °C. XRD investigation on Na_2SO_4:$CaSO_4$ mixtures was conducted on samples synthesised by solid-state reaction. The stoichiometric amount of anhydrous Na_2SO_4 and $CaSO_4$ were thoroughly mixed, grinded in an agate mortar and heated up to temperatures ranging from 800 to 900 °C for 60–100 h in a sealed quartz ampoule. During that time the heating was briefly interrupted (2–3 times) to regrind the charges; the final powder was analysed by X-ray diffraction.

3. Thermodynamic modelling

3.1. Thermodynamic data of stochiometric compounds

The thermodynamic dataset employed for the pure compounds is summarised in Table 2. It includes standard enthalpies of formation, $\Delta H^0_{298,f}$, and standard entropies, S^0_{298}, and temperature-dependent heat capacities, C_p(T), for pure solid and liquid compounds, and the transition temperatures and enthalpies associated with solid-solid and solid-liquid transformations. Thermodynamic data of NaCl, $CaCl_2$, Na_2SO_4 and $CaSO_4$ in the current database were originally extracted from the SGPS database [36] and from the previous reassessments [16,19,26]. Thermodynamic data on double sulphates of sodium and calcium are modelled in this work and detailed in Section 4.2.3. The heat capacity C_p of stoichiometric compounds is modelled as a function of temperature by means of polynomial expansions [37], as given in Eq. (2).

$$C_p = A + B\cdot T + C\cdot T^{-2} + D\cdot T^2 + E\cdot T^3 + \ldots \quad (2)$$

3.2. Thermodynamic model for liquid phase

The liquid phase in the system was described using the modified non-ideal associate species model proposed by Besmann et al. [24], which has demonstrated applicability to complex oxide and salt liquids, e.g. in [25,26,28]. The pure liquid salts, chlorides and sulphates, were considered as solution components, with their mutual interactions governing the thermodynamic behaviour of the liquid phase. In line with the methodology of Besmann et al. [24], each associate species was assigned a total of two non-oxygen atoms per formula unit, thereby ensuring uniform entropic contributions in the ideal mixing term of the database. This approach was adopted to ensure consistency with the general oxide-salt database GTOx [29].

The molar Gibbs energy of the solution is expressed as the sum of three contributions: a reference term, an ideal mixing term, and an excess term accounting for binary interactions, as follows:

$$G_m = \sum x_i {}^{\circ}G_i + RT\sum x_i ln x_i + \sum\sum_{i<j} x_i x_j \sum_{\nu=0} L_{ij}^{(\nu)}\left(x_i - x_j\right)^{\nu} \quad (3)$$

where x_i is the mole fraction of phase constituent i (including the associate species), ${}^{\circ}G_i$ is the molar Gibbs energy of the pure (liquid) phase constituent i and $L_{ij}^{(\nu)}$ with $\nu = 0, 1$ are the interaction coefficients between components i and j, according to the Redlich-Kister polynomial. ${}^{\circ}G_i$ and $L_{ij}^{(\nu)}$ are temperature dependent in the same way, as expressed by the following equation:

$${}^{\circ}G_i, L_{ij}^{(\nu)} = A + BT + CTln(T) + DT^2 + ET^3 + F\Big/T \quad (4)$$

In Eq. (4), only the coefficients A and B are primarily considered and optimised.

3.3. Thermodynamic models for solid solutions

In the present work three solid solubilities are considered in the reciprocal system Na^+, Ca^{2+} // Cl^-, SO_4^{2-}: AlkCl(ss), Na-ortho-MT and HEXA, based on NaCl, Na_2SO_4 (medium-temperature modification), Na_2SO_4 (high-temperature modification), respectively. All solutions are modelled using the compound energy formalism [38].

The description of the sulphate phases was adopted from the previous assessment [19]. The limited solid solubilities in the system Na_2SO_4-$CaSO_4$ was described according to formula proposed by [18] and applied for the complex sulphate system Na^+, K^+, Mg^{2+}, Ca^{2+} // SO_4^{2-} [19], which is: $(Na^{1+}, Ca^{2+}, Va^0)_2(SO_4^{2-})_1$. With the introduction of vacancies on the cation sublattice, Du [18] was able to maintain electroneutrality. The molar Gibbs energy of Na-ortho-MT and HEXA is expressed as follows:

$$G_m = y^I_{Na^{1+}}\,{}^{\circ}G_{Na_2SO_4} + y^I_{Ca^{2+}}\,{}^{\circ}G_{Ca_2SO_4^{2+}} + y^I_{Va^0}\,{}^{\circ}G_{VaSO_4^{2-}} + 2RT\left(y^I_{Na^{1+}} ln y^I_{Na^{1+}} + y^I_{Ca^{2+}} ln y^I_{Ca^{2+}} + y^I_{Va^0} ln y^I_{Va^0}\right) + G^{ex}_m \quad (5)$$

The molar excess Gibbs energy G^{ex}_m is expressed as:

$$G^{ex}_m = y^I_{Me1}\cdot y^I_{Me2}\cdot\sum_{k=0}^{n} L^k_{(Me1,Me2:SO_4^{2-})}\left(y^I_{Me1} - y^I_{Me2}\right)^k \quad (6)$$

where $Me1$ and $Me2$ are the interacting cations (Na and Ca), respectively, Va the vacancies on the first sublattice, and $L^k_{(Me1,Me2:SO_4^{2-})}$ the interaction parameters between cations and vacancies. The term ∘

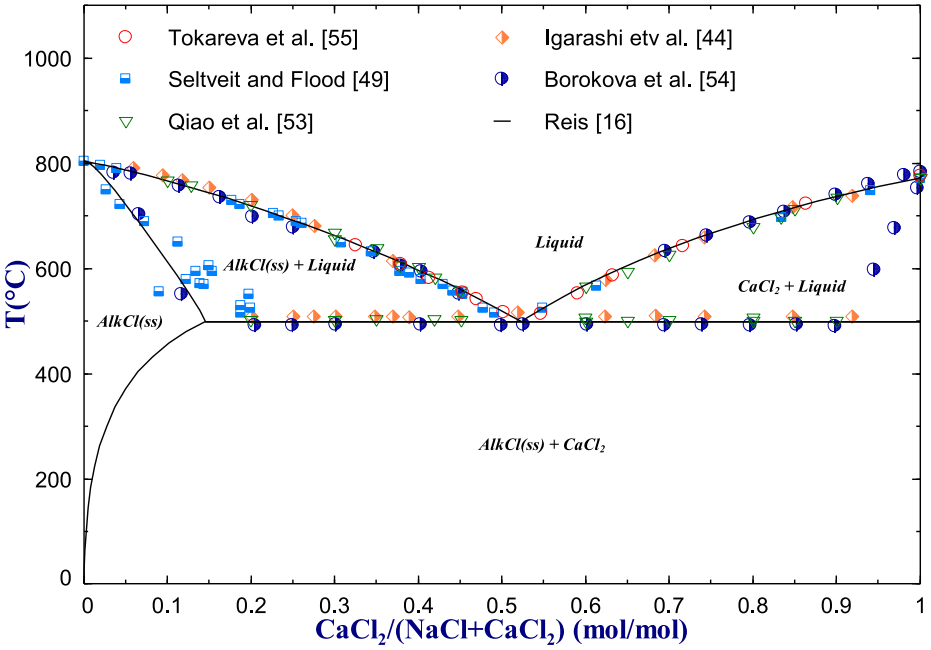

Fig. 1. Phase diagram of NaCl-$CaCl_2$ system from Reis [16] with experimental data: Tokareva et al. [55], Seltveit and Flood [49], Qiao et al. [53], Igarashi et al. [44] and Borovkova et al. [54].

Table 3
Thermal treatment conditions of synthesis of Na_2SO_4(100-x mol%)-$CaSO_4$(x mol %).

Composition	Thermal treatment (heating rate 5 K/min)		
	A	B	C
Na_2SO_4(88 mol%)-$CaSO_4$(12 mol %)	800 °C; 72 h	800 °C; 72 h	
Na_2SO_4(75 mol%)-$CaSO_4$(25 mol %) i.e., $Na_6Ca(SO_4)_4$	800 °C; 60 h	800 °C; 100 h	900 °C; 72 h *
Na_2SO_4(67 mol%)-$CaSO_4$(33 mol %) i.e., $Na_4Ca(SO_4)_3$	800 °C; 72 h	800 °C; 72 h	
Na_2SO_4(50 mol%)-$CaSO_4$(50 mol %) i.e., $Na_2Ca(SO_4)_2$	900 °C; 60 h	850 °C; 72 h	

*quenched in air.

$G_{Na_2SO_4}$ refers to the Gibbs energy of pure Na_2SO_4 (medium- and high-temperature modifications for the solutions Na-ortho-MT and HEXA, respectively). The term $\circ G_{CaSO_4}$ is related to $CaSO_4$ (low- and high-temperature modifications for Na-ortho-MT and HEXA, respectively), and has been optimised in the previous work, as indicated in chapter 5. The $\circ G$ of $Va_2SO_4^{2-}$ was set to be zero as customary in such case. The interaction parameters in both phases $L^k_{(Me1,Me2:SO_4^{2-})}$ in the above equations were re-optimised, according to the phase diagram information for this binary system.

The AlkCl(ss) solution is modelled as $(Na^{1+},Ca^{2+},Va^0)(Cl^-)$ using the sublattice formalism introduced by Reis [16]. Reis [16] described the solubility of $CaCl_2$ in NaCl by expanding the solid solution of NaCl and KCl (referred to as MCl in [16]), incorporating two additional species in the first sublattice: Ca^{2+} and Va^0, representing the calcium ion and an electroneutral vacancy, respectively. In that model, each molecule of $CaCl_2$ was assumed to dissociate into $CaCl^+$ and $VaCl^-$, ensuring the solution remains electroneutral. The molar Gibbs energy of AlkCl(ss) solution is described in a form analogous to Eqs. (5–6), as given by the following expression:

$$G_m = y^I_{Na^{1+}} \circ G_{NaCl} + y^I_{Ca^{2+}} \circ G_{CaCl} + y^I_{Va^0} \circ G_{VaCl^-} + RT\left(y^I_{Na^{1+}} \ln y^I_{Na^{1+}} + y^I_{Ca^{2+}} \ln y^I_{Ca^{2+}} + y^I_{Va^0} \ln y^I_{Va^0}\right) + y^I_{Me1} \cdot y^I_{Me2} \cdot \sum_{k=0}^{n} L^k_{(Me1,Me2:Cl^-)} \left(y^I_{Me1} - y^I_{Me2}\right)^k \quad (7)$$

The interaction parameters for the AlkCl(ss) solid solution in the NaCl-$CaCl_2$ system were optimised based on the phase equilibria data.

3.4. Assessment of Gibbs energy parameters

The thermodynamic assessment of the systems considered in this work was constructed by jointly exploiting newly generated experimental data and selected literature information related to phase diagrams and thermodynamic properties. The modelling procedure started with the generation of the Gibbs energy descriptions for the stoichiometric compounds of the system Na_2SO_4-$CaSO_4$. Prior to parameter optimisation, the C_p functions of all substances were evaluated and subsequently kept fixed. The binary interaction parameters ($L^{(\nu)}_{ij}$) for both liquid and solid phases were then optimised within the binary subsystem in order to reproduce the available thermodynamic data and phase equilibria. On this basis, the binary system NaCl-Na_2SO_4 was then modelled using the available data in literature. Building upon these assessments, the complete reciprocal system was thermodynamically assessed considering the present experimental results along with the data available from the literature. Parameter optimisation was carried out using the Calphad Optimizer module [39] implemented in the FactSage software [40,41], using a dataset composed of both literature information and experimental results generated in this study.

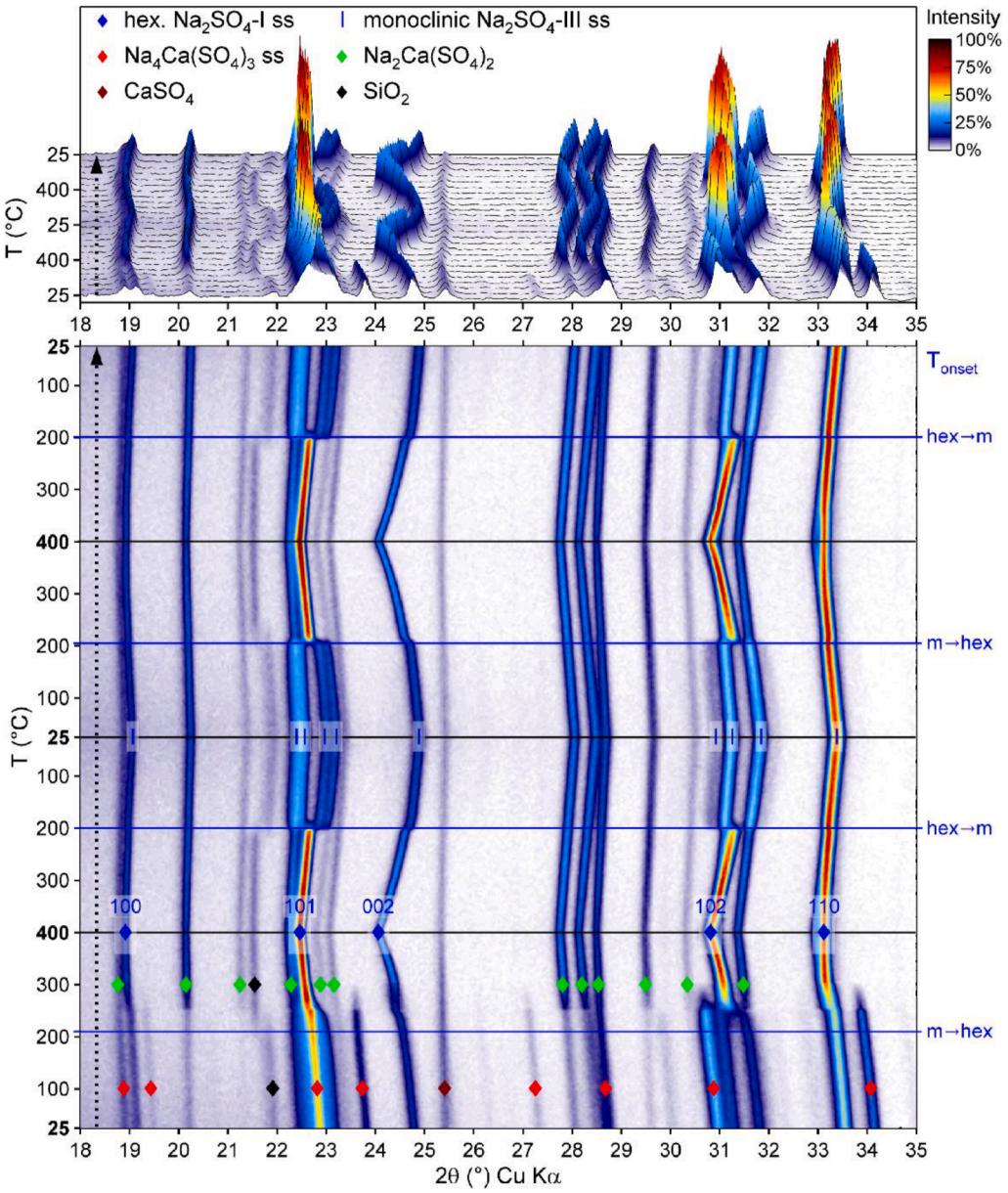

Fig. 2. High temperature X-ray diffractogram of Na_2SO_4(75 mol%)-$CaSO_4$(25 mol%).

4. Results and discussion

The following section presents the results of the experimental campaign and thermodynamic modelling performed for the investigated subsystems. The results and related discussion are organised into subsections, each combining the experimental findings with the corresponding thermodynamic assessment. When a given subsystem required further investigation by means of complementary techniques in support of its thermodynamic description, the corresponding subsection was further divided into dedicated sub-subsections.

4.1. *NaCl-$CaCl_2$*

The phase diagram of the system NaCl-$CaCl_2$ has been thoroughly investigated using thermal analysis and X-ray diffraction [44–55]. Menge [45] and Seltveit and Flood [49] reported the presence of an intermediate compound Na_4CaCl_6, but other research disputed this, instead highlighting a significant solubility of $CaCl_2$ in solid NaCl, reaching up to 20 mol% $CaCl_2$ [49,54]. The eutectic composition is estimated to fall within the range of 51 to 53 mol% $CaCl_2$, with the eutectic temperature reported to vary, showing values around 492 °C [54], 500 °C [53], 506 °C [56] and 510 °C [44]. Østvold [57] conducted heat of mixing measurements at 10 mol% intervals, whereas Sem et al. [58] collected data at larger intervals of around 25 mol%. Despite the difference in measurement intervals, the results from both studies were in good agreement. Østvold [57] and Egan and Bracker [59] reported consistent results for the NaCl activity in the liquid phase, even though their measurements were taken at temperatures differing by 25 °C. Solubility of NaCl in $CaCl_2$ has only been reported by Borovkova et al. [54]. Based on available experimental data, the phase diagram was calculated and optimised by Chartrand and Pelton [14], Yin et al. [15] and Reis [16]. As outlined in Section 3.3, Reis [16] described the solubility of $CaCl_2$ in NaCl by expanding the solid solution of NaCl and KCl, referred to as MCl. The obtained parameters for liquid and solid phases [16] are used in the current work (Table 9), allowing a good description of phase equilibria (Fig. 1) and the activity of NaCl in the liquid phase. The final eutectic transition was calculated at 52.35 mol% $CaCl_2$ with a temperature of 499 °C and enthalpy of fusion of 16.34 kJ/mol. The

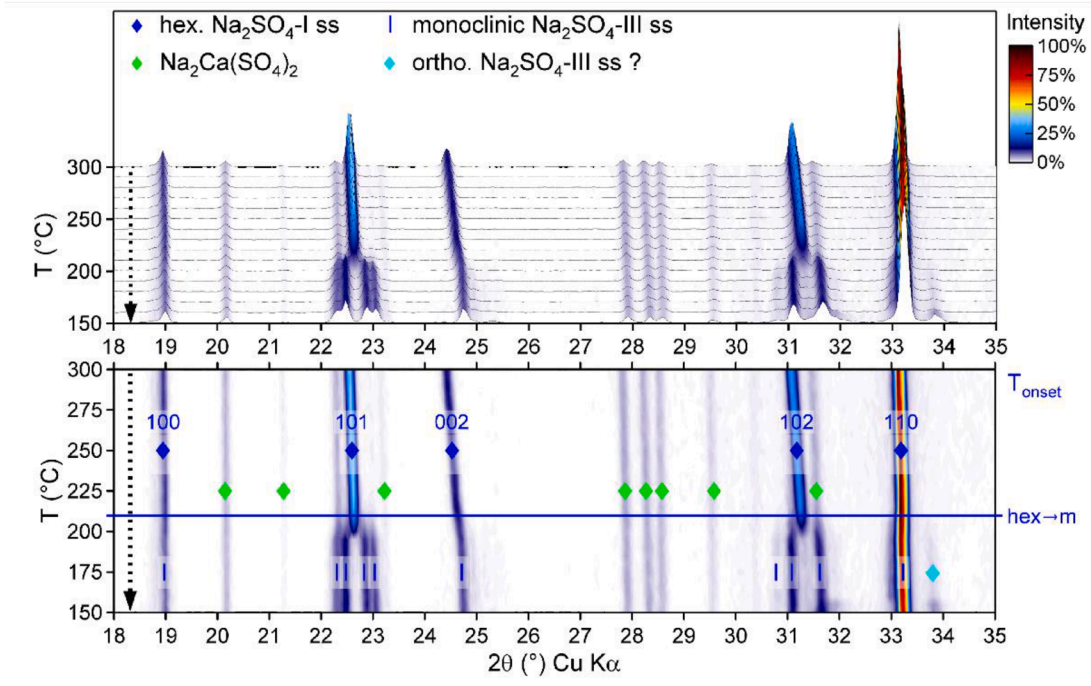

a

Fig. 3. High temperature X-ray diffractogram of Na_2SO_4(88 mol%)-$CaSO_4$(12 mol%) mixture: **a** HT1; **b** HT3; **c** HT4.

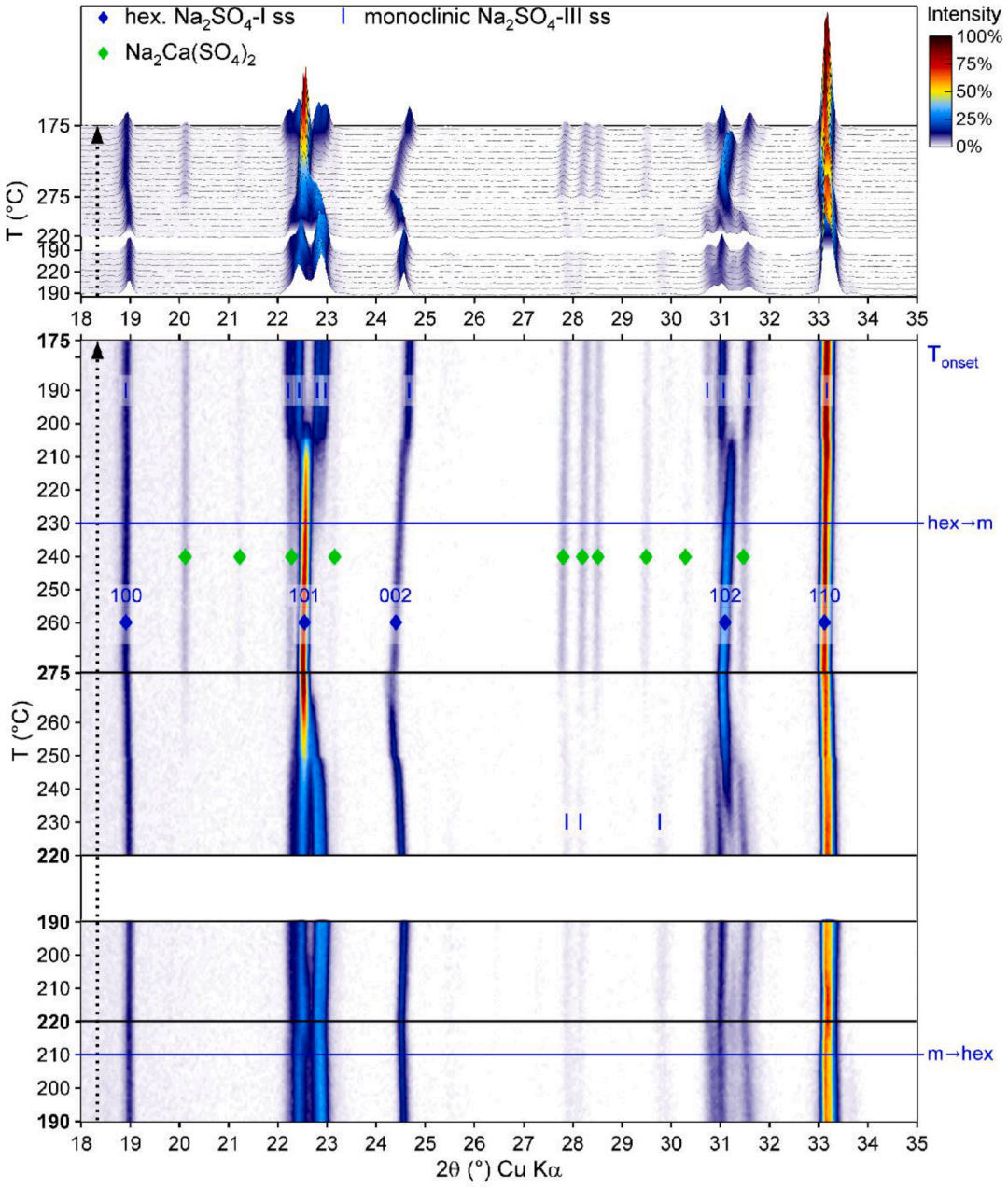

b

Fig. 3. (*continued*).

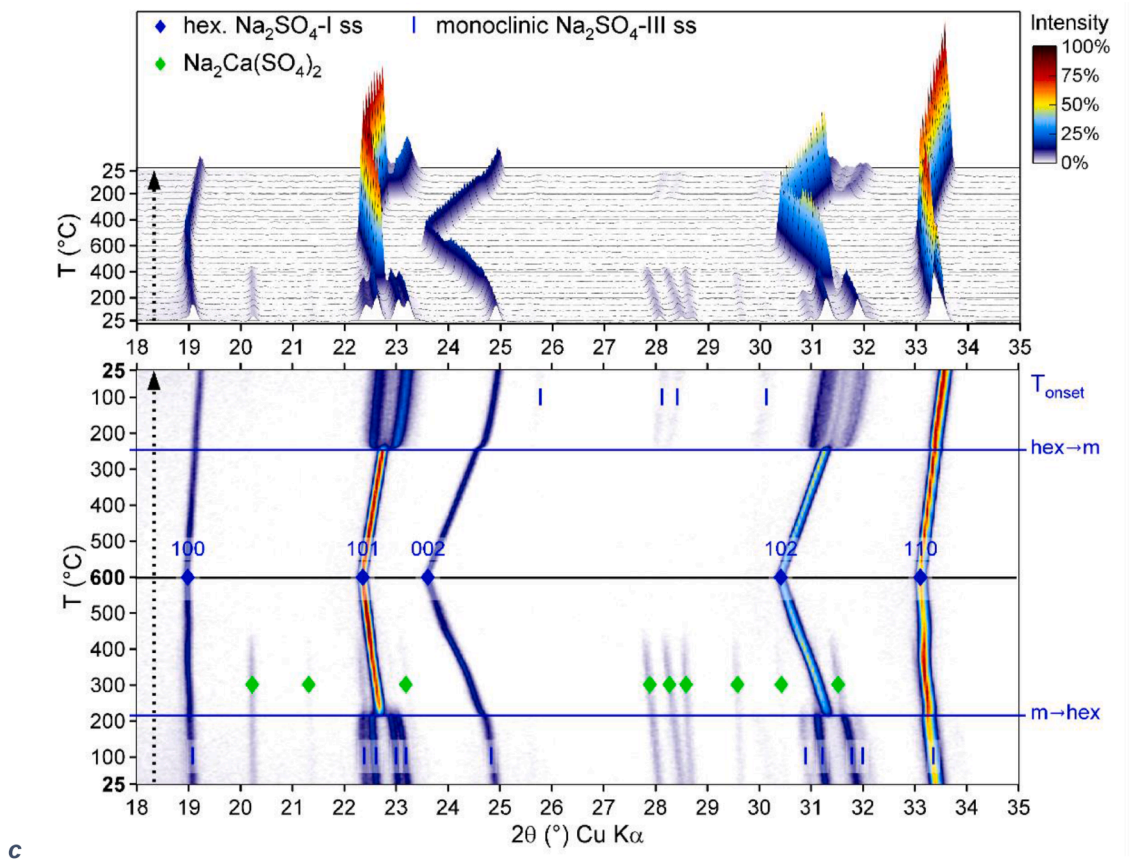

Fig. 3. (*continued*).

evaluation performed by Reis [16] has been integrated into the construction of the database utilised in this study.

4.2. Na_2SO_4-$CaSO_4$

The phase diagram was previously experimentally investigated [9,11–13,17,60–66] and assessed [18,19]. The challenges and discrepancies in describing such a binary system arise from the presence and nature of intermediate compounds. Kommissarova et al. [63] and Freyer et al. [60,66] reported the compound with Na_2SO_4-$CaSO_4$ ratio 1:1 ($Na_2Ca(SO_4)_2$), known as glauberite. Müller [61] found a compound with Na_2SO_4-$CaSO_4$ ratio 4:1 as a result of melt segregation, along with $CaSO_4$. Kobertz et al. [11] confirmed the impossibility of forming glauberite by crystallisation from the melt, but a compound with Na_2SO_4-$CaSO_4$ ratio 3:1 was found as result of segregation event, instead of 2:1 ratio. The existence of the compound with composition 3:1, $Na_6Ca(SO_4)_4$, was confirmed by XRD analysis of four compositions (18, 22, 78 and 82 mol% $CaSO_4$) under different heat treatment [11]. Their XRD investigations found two compounds with compositions Na_2SO_4-$CaSO_4$ 3:1 and 1:1 and no significant solubility of calcium in the solid high temperature-Na_2SO_4 (Na_2SO_4-HT) was detected compared to other studies [12,13].

Eysel et al. [67] investigated the crystal chemistry and structures of Na_2SO_4 and its solid solutions, including the Na_2SO_4-$CaSO_4$ system. Four solid solution phases were described, namely the hexagonal high-temperature solid solution phase with Na_2SO_4-I crystal structure (structure type: α-K_2SO_4(HT), space group: P63/mmc, e.g. ICSD collection code 81,503) and three sodium-rich solid solution phases: the orthorhombic medium temperature solid solution phase with Na_2SO_4-III crystal structure (space group Cmcm, lattice parameters of pure Na_2SO_4 at room temperature: a = 5.6274 Å, b = 8.9664 Å, c = 9.9737 Å, and V = 354.88 $Å^3$ (ICSD 66,554)) and two phases with crystal structures related to the orthorhombic Na_2SO_4-III, but with a slight monoclinic distortion. One monoclinic solid solution phase with the approximate chemical composition $(Na_{0.9}Ca_{0.05})_2SO_4$ is reported with following lattice parameters at room temperature: a ≈ 9.27 Å, b ≈ 5.35 Å, c ≈ 7.12 Å, β ≈ 92.4° and V ≈ 352.5 $Å^3$ (ICDD PDF 29-1291 (Zn-stabilised)). The other sodium-rich solid solution phase with the approximate chemical composition $(Na_{0.8}Ca_{0.1})_2SO_4$ has a different monoclinic angle, which is now α instead of β. Its lattice parameters at room temperature are as follows: a ≈ 9.25 Å, b ≈ 5.34 Å, c ≈ 7.13 Å, α ≈ 91.4° and V ≈ 352.0 $Å^3$ (ICDD PDF 29-1296). The exact crystal structure of the two monoclinic phases is not known yet.

Freyer et al. [60] examined the Na_2SO_4-$CaSO_4$ system, focusing on the formation and transformation of metastable solid solutions obtained through quenching of molten mixtures and their conversion into stable phases. Samples ranged from freshly quenched molten mixtures to long-term annealed solids, allowing for an in-depth analysis of phase stability. Using X-ray diffraction and differential thermal analysis, the authors provided detailed insights into the structural and thermal properties of the system across varying compositions and temperatures. The findings highlighted glauberite (Na_2SO_4·$CaSO_4$) as the only stable compound in the system, existing up to 520 °C, beyond which it decomposes. Thenardite (Na_2SO_4 V, low-temperature modification) was identified as a stable phase at low temperatures, while the hexagonal Na_2SO_4 I phase (high-temperature modification) represents the sole stable solid solution. The thermal effects observed between 230 °C and 280 °C were attributed to reproducible transformations between hexagonal and monoclinic lattice structures within the metastable region of the phase diagram, challenging earlier interpretations [12,13,64] that these effects corresponded to equilibrium transformations. The study identified three metastable solid solutions, whose formation depends on the $CaSO_4$ content. Solid solution A, consisting of up to 4 mol% $CaSO_4$, is associated with stabilised Na_2SO_4 III (orthorhombic,

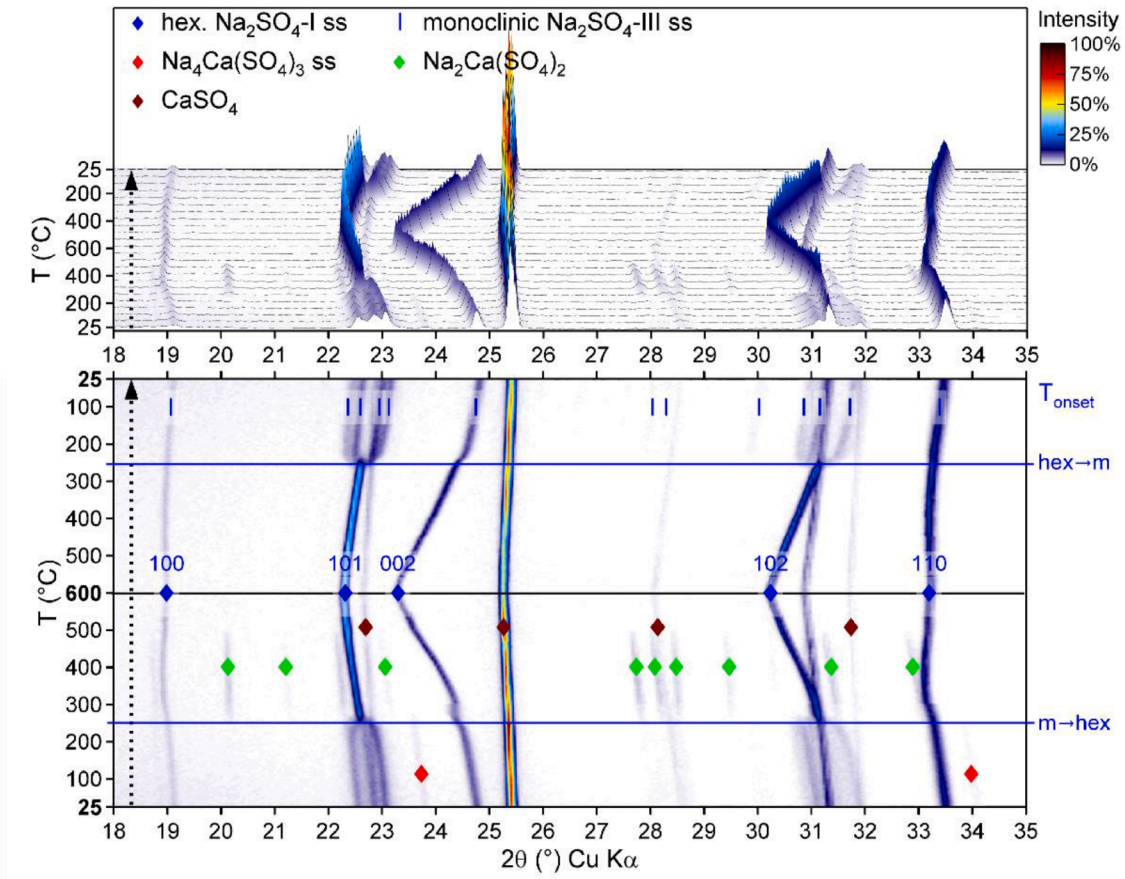

Fig. 4. High temperature X-ray diffractogram of Na_2SO_4(50 mol%)-$CaSO_4$(50 mol%) mixture (HT1).

Table 4
Onset temperatures of the monoclinic/hexagonal phase transition.

Composition	Experiment conditions		T_{onset} (°C)
Na_2SO_4(75 mol%)-$CaSO_4$(25 mol%) C	HT1, Cycle 1	25 °C → 400 °C	210
	HT1, Cycle 1	400 °C → 25 °C	200
	HT1, Cycle 2	25 °C → 400 °C	205
	HT1, Cycle 2	400 °C → 25 °C	200
Na_2SO_4(88 mol%)-$CaSO_4$(12 mol%)	HT1	300 °C → 150 °C	210
	HT3abc	190 °C → 220 °C → 190 °C → 275 °C	210
	HT3d	275 °C → 150 °C	230
	HT4a	25 °C → 600 °C	210
	HT4b	600 °C → 25 °C	245
Na_2SO_4(50 mol%)-$CaSO_4$(50 mol%) B	HT1	25 °C → 600 °C	250
	HT1	600 °C → 25 °C	260

middle-temperature modification), while solid solution B, containing between 4 and 20 mol% $CaSO_4$, corresponds to the two phases with monoclinic distorted Na_2SO_4-III structure, which were consolidated by Freyer et al. [60] as one phase, called stabilised Na_2SO_4 I. Solid solution C, comprising between 33 and 40 mol% $CaSO_4$, is identified as a metastable phase resembling $2Na_2SO_4{\cdot}CaSO_4$. The study determined the limiting concentrations of $CaSO_4$ for these metastable phases and proposed a transformation scheme describing their conversion into stable phases, with glauberite and thenardite predominating at low temperatures. The crystal structure of solid solution C, $Na_4Ca(SO_4)_3$, was later published by Shablinskii et al. [68] (trigonal, space group R3, lattice parameters: a = 15.7278 Å, c = 22.0037 Å, V = 4713.7 $Å^3$, ICSD 143, 077).

Kobertz et al. [11] conducted a detailed reinvestigation of the phase diagram using Differential Thermal Analysis and X-ray Diffraction. Their DTA study comprised 15 measurements performed in Al_2O_3 crucibles in air, 13 measurements conducted in sealed quartz crucibles under vacuum conditions ($<10^{-1}$ mbar) at temperatures below 1200 °C, 5 measurements in open Al_2O_3 crucibles with a gas mixture containing 14 vol % CO_2, 6 vol% O_2, 2 vol% SO_2, and the balance N_2, and 12 measurements carried out in Pt crucibles with lids in air. $Na_6Ca(SO_4)_4$ was found to melt congruently at 950 °C and to take part in two eutectic reactions with eutectic points at 46 mol% $CaSO_4$ and 925 °C and at 1–2 mol% $CaSO_4$ and 882 °C. $Na_2Ca(SO_4)_2$ was reported to decompose peritectoidally into $Na_6Ca(SO_4)_4$ and $CaSO_4$ at 910 °C.

The phase diagram was assessed by Du [18] and Yazhenskikh et al. [19]. Unlike Du's work [18], Yazhenskikh et al. [19] included in their assessment double sulphates, with composition 1:1 and 3:1, $Na_2Ca(SO_4)_2$ and $Na_6Ca(SO_4)_4$, the latter based on the experimental findings of Kobertz et al. [11]. The assessment conducted by Yazhenskikh et al. [19] was mainly performed based on the experimental data of Kobertz et al. [11] and provides optimised thermodynamic properties of double

Table 5
Semiquantitative evaluation of investigated samples.

Sample (mol% $CaSO_4$ & heat treatment)	Conditions	Na_2SO_4-III	$(Na_{0.9}Ca_{0.05})_2SO_4$	$(Na_{0.8}Ca_{0.1})_2SO_4$	$Na_4Ca(SO_4)_3$	$Na_2Ca(SO_4)_2$	$CaSO_4$
12	25 °C, as-prepared	-	+++	?		–	
12	150 °C / vacuum, slowly cooled from 300 °C (HT1)	–?	+++			+	
12	25 °C / synthetic air, slowly cooled from 150 °C (HT2)	-?	+++			-	
12	175 °C, fast cooled from 500 °C to 70 °C (HT2)	–?	++	++			
12	25 °C, slowly cooled from 275 °C (HT3d)		+++			+	
12	25 °C, slowly cooled from 600 °C (HT4)		++	++			
25 A	25 °C, as-prepared	+	+	?		–	+
25 B	25 °C, as-prepared		+	?	+	+	–
25 C	25 °C, as-prepared		++	?	+	-	–
25 C	25 °C, after two cycles with T_{max}=400 °C		+			+	–
33 A	25 °C, as-prepared		++	?	-	-	+
33 B	25 °C, as-prepared		++	?	-	-	+
50 A	25 °C, as-prepared		-	?	-	–	++
50 A + B	25 °C, as-prepared			++	–		++
50 A + B	25 °C, slowly heated to 600 °C, slowly cooled to 25 °C		++	?			++

"–" <10 wt%; "-" =10–20 wt%; "+" =20–40 wt%; "++" =40–60 wt%; "+++" >60 wt%; "?" phase identification questionable (Na_2SO_4-III: absence of distinct non-overlapping reflections; $(Na_{0.8}Ca_{0.1})_2SO_4$: unambiguous identification due to peak overlap with $(Na_{0.9}Ca_{0.05})_2SO_4$).

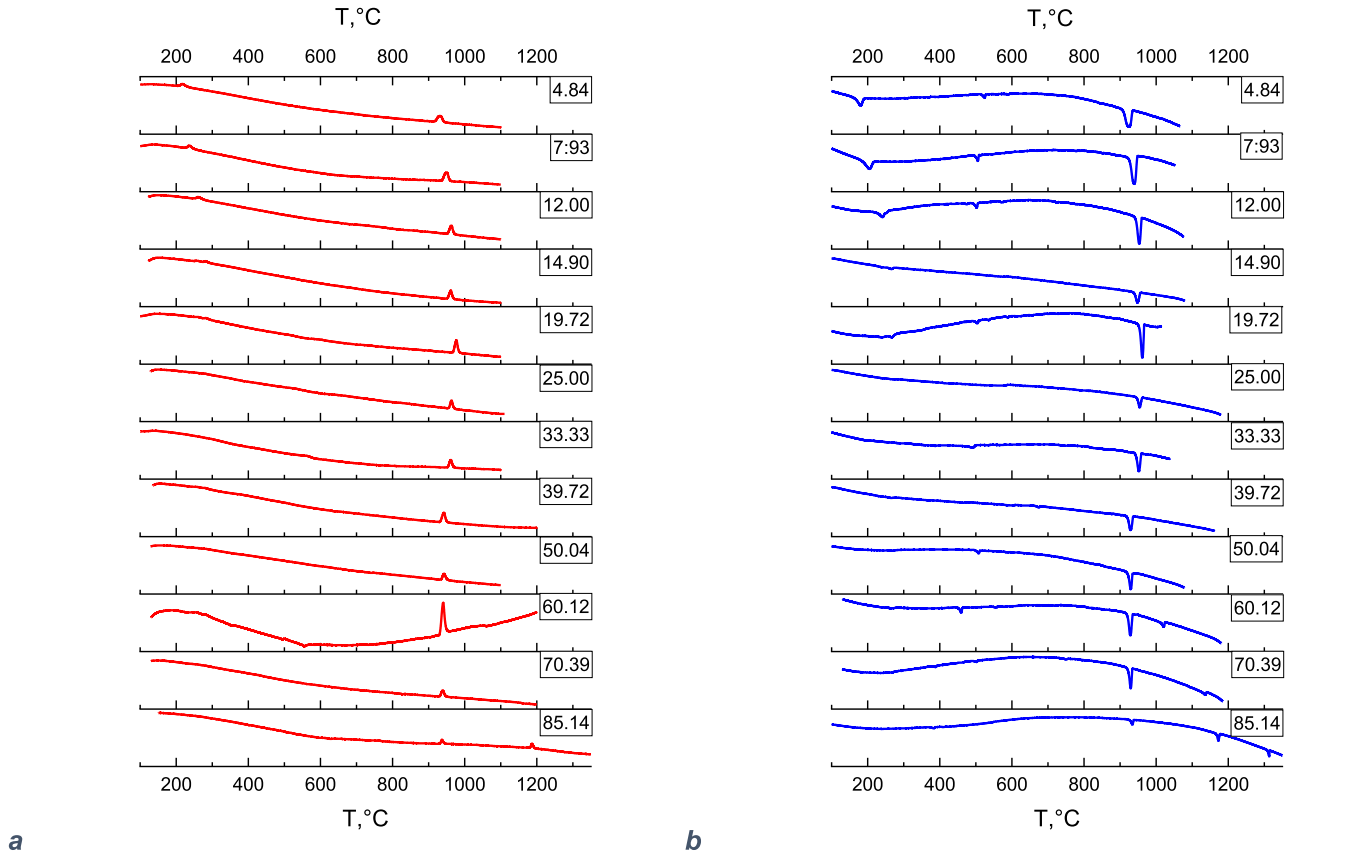

Fig. 5. DTA curves of Na_2SO_4-$CaSO_4$ mixtures, expressed in molar percentage of $CaSO_4$: a heating curves; b cooling curves.

sulphates. The heat capacity data were generated from the corresponding data of pure sulphates by using Neumann-Kopp rule and/or based on calorimetric data [66]. According to the latest assessment [19], the intermediate compound $Na_6Ca(SO_4)_4$ undergoes congruent melting at 949.2 °C and participates in two eutectic reactions. The first occurs with Na_2SO_4 (HT) at 2 mol% $CaSO_4$ and 882.7 °C, while the second involves $CaSO_4$ at 50.4 mol% $CaSO_4$ and 925.6 °C.

To validate existing experimental data, resolve discrepancies in the literature, and obtain information on potential intermediate compounds, the present study employs a combined investigation using DTA, DSC, and HT-XRD.

4.2.1. XRD/HT-XRD

Four Na_2SO_4-$CaSO_4$ mixtures (12.0, 25.0, 33.3, and 50.0 mol%

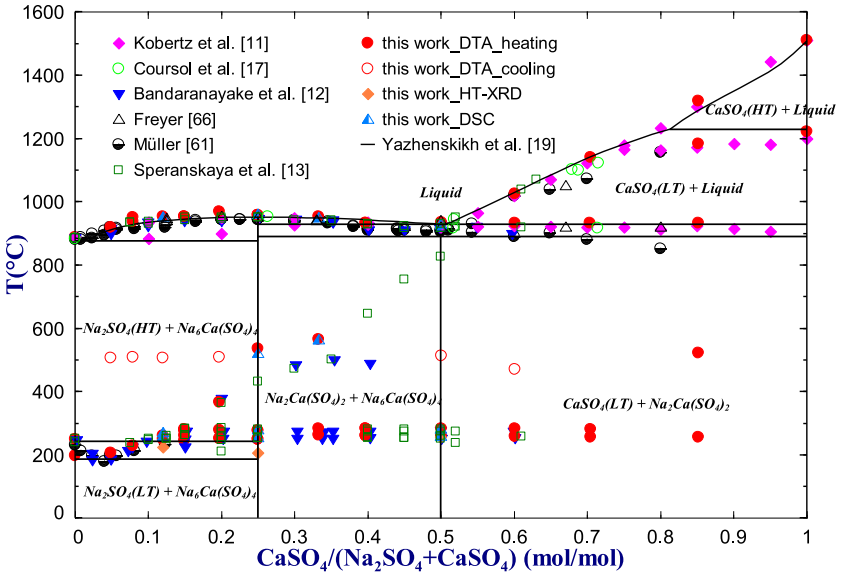

Fig. 6. Phase diagram of Na_2SO_4-$CaSO_4$ system calculated in Yazhenskikh et al. [19] with experimental data: this work and Kobertz et al. [11], Coursol et al. [17], Bandaranayake et al. [12], Freyer [66], Müller [61], Speranskaya et al. [13].

Table 6
Transition temperatures and enthalpies of Na_2SO_4-$CaSO_4$ mixtures from DSC experiments (heating curves) at pressure P = 0.1 MPa.

	1		2		3		4	
$CaSO_4$, mol%	T, °C	ΔH, kJ/mol	T, °C	ΔH, kJ/mol	T, °C	ΔH, kJ/mol	T, °C	ΔH, kJ/mol
12.0	259	2.8 ± 0.5					950	15.1 ± 0.9
25.0	253	0.14 ± 0.09	278	0.53 ± 0.06	519	3.43 ± 0.09	959	18.8 ± 0.7
33.3					562	8.22 ± 0.06	948	19.3 ± 1.0
50.0	258	0.13 ± 0.01	281	0.3 ± 0.2			929	18.9 ± 0.6

u(mol%) = 0.03 mol%; u(T) = 1.2 °C; u(P) = 5 kPa.
Uncertainties associated with the enthalpy values are given as the standard deviation of replicate measurements.

$CaSO_4$) were synthesised in situ and subjected to XRD investigation. The mixtures were meticulously prepared by combining the end-members in their appropriate stoichiometric ratios. This was achieved through solid-state reaction, starting with the grinding of the pure compounds in an agate mortar in a glovebox, placing the resulting mixture in quartz ampoules, and sealing them under vacuum using a hydrogen/oxygen flame. The ampoules were then heated in a furnace at specified temperatures below the melting point, generally under 1000 °C, to prevent the quartz walls from fracturing. After heating, the ampoule was opened in a glovebox, the mixture was recovered, ground again in a mortar, and transferred to a new quartz ampoule, which was subsequently sealed for additional iterative stages (A, B, C). They are summarised in Table 3. The thermal history appeared to play a crucial role in forming the desired mixture, as demonstrated by XRD tests conducted at intermediate stages, which revealed the presence of pure phases in varying proportions (Tables S 1–4). XRD analyses were performed both at room temperature and at high temperatures. RT-XRD measurements were conducted on four compositions, while HT-XRD were carried out on three of them. The results of the high-temperature XRD analyses are presented in this work, while room temperature data are provided in the supplementary section (Figures S 1–4).

After synthesis, a combination of three to five of the following six phases was always observed at room temperature: orthorhombic Na_2SO_4-III, the two monoclinic Na_2SO_4-III solid solution phases $(Na_{0.9}Ca_{0.05})_2SO_4$ and $(Na_{0.8}Ca_{0.1})_2SO_4$, $Na_4Ca(SO_4)_3$, $Na_2Ca(SO_4)_2$ and $CaSO_4$.

To track the formation of the phases, the high-temperature X-ray diffraction measurements were conducted for the samples Na_2SO_4(100-x mol%)-$CaSO_4$(x mol%) with x = 12, 25 and 50. Specifically, 3D surface plots with projections are used to visualise the data. The Bragg reflections of the hexagonal high temperature solid solution phase Na_2SO_4-I are marked with blue diamonds ♦ and the according hkl index. On cooling, this phase transforms to the monoclinic $(Na_{0.9}Ca_{0.05})_2SO_4$ solid solution phase or $(Na_{0.8}Ca_{0.1})_2SO_4$ solid solution phase or a mixture of both (apparently depending on cooling conditions). The hexagonal 101 and 102 reflections split then into three to four reflections (see Supplementary, Figures S 5–6). The reflections of the monoclinic phase are marked with |. For other phases, only the strongest reflections with low peak overlapping are marked as follows: $Na_2Ca(SO_4)_2$ with ♦, $Na_4Ca(SO_4)_3$ with ♦, Na_2SO_4-III with ♦ and $CaSO_4$ with ♦.

The mixture Na_2SO_4(75 mol%)-$CaSO_4$(25 mol%) "C" was analysed by XRD at high temperature. Two cycles of heating from 25 °C to 400 °C and cooling to 25 °C were performed in synthetic air (Fig. 2 and Figure S 5). Fast scans (2 min overall measurement time) were performed at 5 K intervals, long scans (1 h overall) at 50 K intervals. Between scans, a heating/cooling rate of 2 K/min was applied, which, taking in account

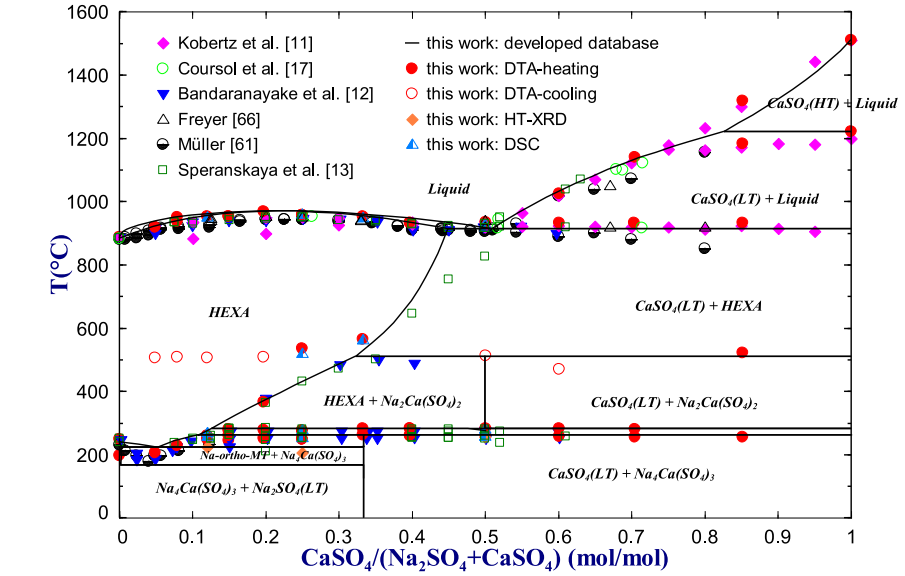

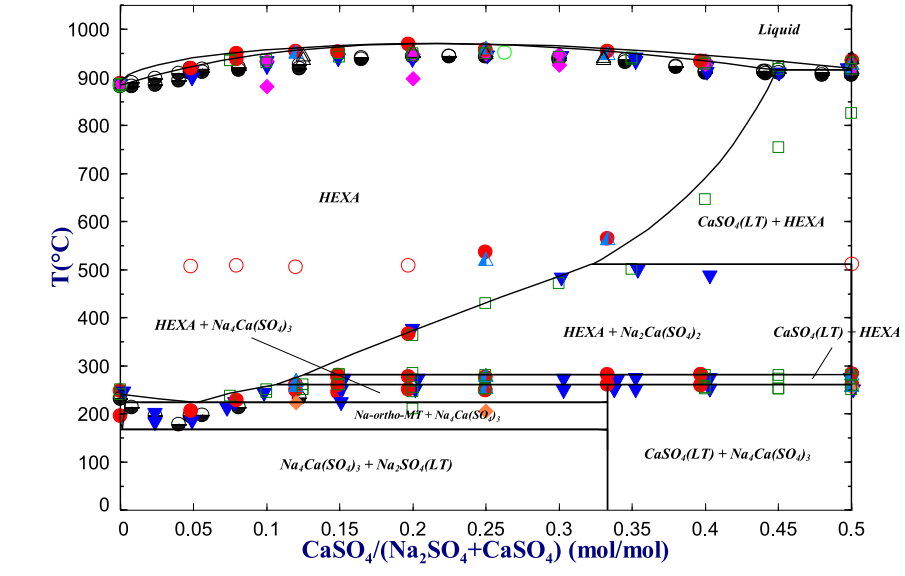

Fig. 7. Phase diagram of Na_2SO_4-$CaSO_4$ system: a comparison of the developed database with experimental data from this work and Kobertz et al. [11], Coursol et al. [17], Bandaranayake et al. [12], Freyer [66], Müller [61], Speranskaya et al. [13]; b zoomed-in view of the phase diagram in the Na_2SO_4-rich region.

short scans, resulted in a rate of 1 K/min and a dwell time of 1 h every 50 K. The sample initially consisted of the monoclinic $(Na_{0.8}Ca_{0.1})_2SO_4$ solid solution phase, $Na_4Ca(SO_4)_3$, $Na_2Ca(SO_4)_2$, $CaSO_4$ and a small amount of Cristobalite (SiO_2, residual of a quartz ampoule, marked with ♦). Coincidentally, the Cristobalite transformation from the cubic β high temperature modification to tetragonal α occurs at similar temperatures as the transformation of hexagonal to monoclinic solid solution phase.

$Na_4Ca(SO_4)_3$, presumably corresponding to dobrovolskyite [68], was observed in several samples after synthesis (Figures S 2–4). In HT-XRD experiments, it disappeared upon heating during the transformation of monoclinic to hexagonal solid solution phase and did not reappear (Fig. 2).

The room temperature stable phase Na_2SO_4-V (Na-LT, Thenardite, space group Fddd, ICSD 81,506) was occasionally formed after exposure to ambient air for several days (not shown here).

In order to find regular kinetic effects, variations in cooling rates and prolonged annealing times at certain temperature were applied in later experiments.

The mixture Na_2SO_4(88 mol%)-$CaSO_4$(12 mol%) was subjected to four HT-XRD experiments. The first high temperature experiment (HT1, Fig. 3a) was performed under high vacuum. After annealing at 300 °C

Table 7
Invariant points in the Na_2SO_4-$CaSO_4$ system.

Reaction	Reaction type	$CaSO_4$, mol (in Liquid)	T, °C	Ref.
Na_2SO_4(LT)+ $Na_4Ca(SO_4)_3$ ↔ Na-ortho-MT	Eutectoid	appr. 0.003	170	[a]
Na-ortho-MT + $Na_4Ca(SO_4)_3$ ↔ HEXA	Eutectoid	0.04	178	[61]
		0.049	185.81	[12]
		0.052	223	[a]
HEXA ↔ Liquid (maximum)	Azeotrope	0.20	944	[61]
		0.20–0.25	950	[13]
		appr. 0.25	945	[12]
		0.2	952	[66]
		0.25	949.2	[19] [b]
		0.223	970	[a]
HEXA + $CaSO_4$(LT) ↔ $Na_4Ca(SO_4)_3$	Decomposition	0.333	261	[a]
HEXA + $CaSO_4$(LT) ↔ Liquid	Eutectic	0.4	913	[61]
		0.47	909	[12]
		0.49	918	[13]
		0.5	916	[17]
		-	919	[60]
		0.46	925	[11]
		0.504	925.6	[19] [b]
		0.509	915	[a]
HEXA + $CaSO_4$(LT) ↔ $Na_2Ca(SO_4)_2$	Formation	0.5	282	[a]
$Na_2Ca(SO_4)_2$ ↔ HEXA + $CaSO_4$(LT)	Decomposition	0.5	520	[66]
		0.5	910	[11]
		0.5	910.1	[19] [b]
		0.5	507	[a]

[a] this work.
[b] in the work of Yazhenskikh et al. [19], the congruent melting compound $Na_6Ca(SO_4)_4$ is considered instead of the solid solution HEXA.

for 5 h, the sample was cooled to 150 °C with approximately 1 K/min and 1 h annealing (long scans) in 25 K intervals. The atmosphere was switched to synthetic air before cooling to 25 °C. The second experiment (HT2) was a quenching test. The sample was cooled fast from 500 °C to 70 °C by turning off the heater and heated to 175 °C without measurements. The achieved average cooling rates were 30 K/min from 500 °C to 200 °C and 10 K/min from 200 °C to 100 °C. During the following 10 h annealing at 175 °C with continuous measurements the sample barely changed. It consisted of approximately equal amounts of the two monoclinic solid phases $(Na_{0.9}Ca_{0.05})_2SO_4$ and $(Na_{0.8}Ca_{0.1})_2SO_4$ and a small amount of Na_2SO_4-III, which remains questionable. Thereafter, the sample was homogenised. Heated to 175 °C under vacuum and then kept at 175 °C under synthetic air for 5 days. No changes to the sample were observed. Focus of the following experiments (Fig. 3b and Figure S 6) was the behaviour around the hexagonal to monoclinic phase transition. During heating to 220 °C and the following cooling to 190 °C in the first stage of the experiment (HT3a) (0.25 K/min heating/cooling rate and 1 h annealing at 5 K intervals, Figure S 6a) the amount of $(Na_{0.9}Ca_{0.05})_2SO_4$ increased at cost of $(Na_{0.8}Ca_{0.1})_2SO_4$. Although the beginning formation of the hexagonal solid solution phase was already observed at 225 °C in experiment HT3bc (0.25 K/min heating and 1 hour annealing at 250 °C, Figure S 6b), the monoclinic low temperature solid solution phase was still detectable up to 260 °C. Around this point the formation of $Na_2Ca(SO_4)_2$ started. The slow cooling from 275 °C to 150 °C in experiment HT3d (0.25 K/min cooling rate and 1 h annealing at 250 °C, 225 °C, 205 °C, 200 °C, 195 °C, 190 °C, 175 °C, and 150 °C, Figure S 6c) seems to prevent the formation of $(Na_{0.8}Ca_{0.1})_2SO_4$. The hexagonal Na_2SO_4-I transformed only to $(Na_{0.9}Ca_{0.05})_2SO_4$. No change in the content of $Na_2Ca(SO_4)_2$ was observed. During the experiment HT4 (Fig. 3c) the sample was heated from 25 °C to 600 °C and cooled to 25 °C in order to investigate the stability range of $Na_2Ca(SO_4)_2$. During heating (HT4a, 0.8 K/min heating rate, no annealing steps) $Na_2Ca(SO_4)_2$ vanished around 440 °C. However, it was not formed during cooling to 25 °C (HT4b, 1 K/min cooling rate, 1 h annealing at 50 K intervals). The hexagonal Na_2SO_4-I transformed to approximately equal amounts of $(Na_{0.9}Ca_{0.05})_2SO_4$ and $(Na_{0.8}Ca_{0.1})_2SO_4$.

The mixture Na_2SO_4(50 mol%)-$CaSO_4$(50 mol%) was subjected to HT-XRD analysis and 3D plots are illustrated in Fig. 4. Although, $Na_2Ca(SO_4)_2$ was the targeted phase, it was not present in the initial state. It formed in experiment HT1 (25 °C → 600 °C → 25 °C, 0.8 K/min heating/cooling rate, 1 h annealing at 50 K intervals, 2 h annealing at 600 °C) at approximately 250 °C on heating together with formation of Na_2SO_4-I solid solution, but did not form on cooling. A small amount formed again on heating to 400 °C. The sample was kept then for 3 days at 400 °C and 4 days at 300 °C (HT2). The content increased slowly and reached 21 wt % (other phases: 44 wt% Na_2SO_4-I + 36 wt% $CaSO_4$) in the end.

The high-temperature experiments conducted revealed the monoclinic-to-hexagonal phase transition [$(Na_{0.9}Ca_{0.05})_2SO_4$ / $(Na_{0.8}Ca_{0.1})_2SO_4$ ⇆ Na_2SO_4-I] at the onset temperatures specified below for the respective compositions analysed. These values are summarised in Table 4, corresponding to the different thermal cycles or measurements performed.

A summary of the semi-quantitative evaluation of the phases identified in the experiments, conducted at either room temperature or high temperature is provided in Table 5, with estimated weight percentage ranges. While the values offer a useful approximation, they remain subject to potential uncertainties.

The quantifications are made utilising the Rietveld method which requires the crystal structure of each phase. As already mentioned, the actual crystal structures of $(Na_{0.9}Ca_{0.05})_2SO_4$ and $(Na_{0.8}Ca_{0.1})_2SO_4$ are not known, but are assumed [67] to be monoclinic distorted Na_2SO_4-III (Na-MT). Therefore, the crystal structure of the orthorhombic Na_2SO_4-III (ICSD 66,554) was adapted to monoclinic symmetry without changing atomic positions or site occupancies, as the low data quality due to overlaps with other phases does not allow it. This imperfect structural model matches the measured data well enough to enable an at least semiquantitative evaluation. A detailed view on the diffraction patterns of both phases is given in the supplementary section.

A question mark in the $(Na_{0.8}Ca_{0.1})_2SO_4$ column of Table 5 indicates that it might be present together with a larger amount of $(Na_{0.9}Ca_{0.05})_2SO_4$, but peak overlapping prevents a proper identification. A question mark in the Na_2SO_4-III column of Table 5 indicates the absence of distinct, non-overlapping reflections typically associated with this phase. This suggests the possibility of a different, as yet

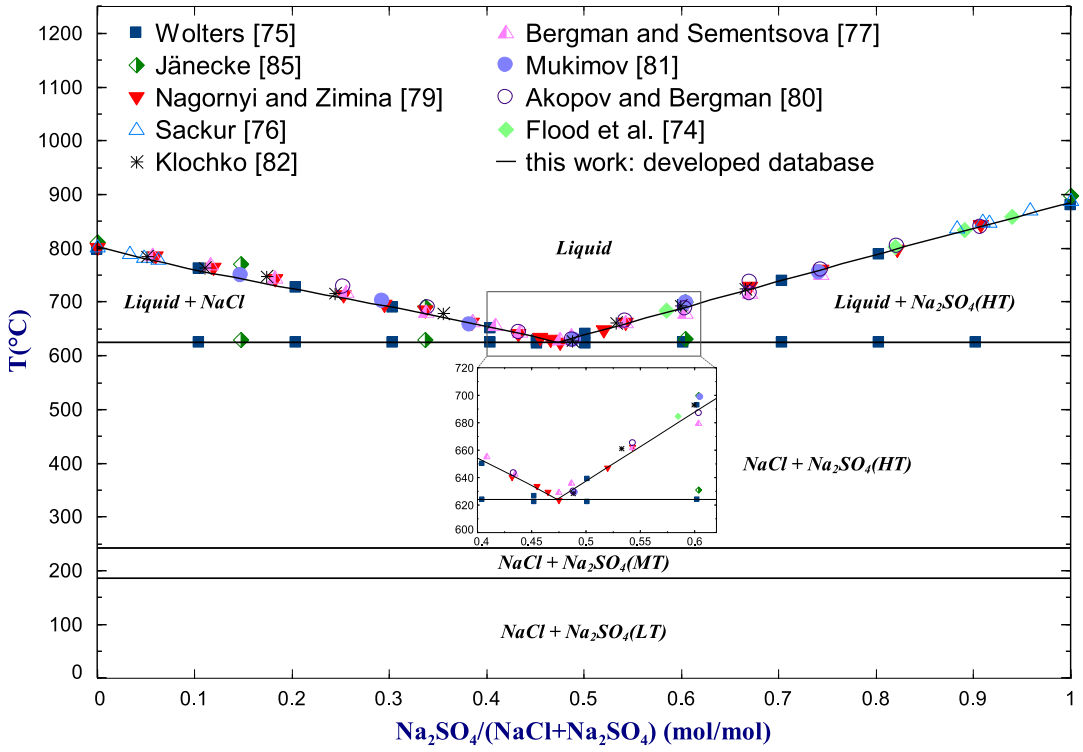

Fig. 8. Phase diagram of NaCl-Na_2SO_4 system: comparison of the developed database with experimental data from Wolters [75], Jänecke [85], Nagornyi and Zimina [79], Sackur [76], Klochko [82], Bergman and Sementsova [77], Mukimov [81], Akopov and Bergman [80], Flood at al [74].

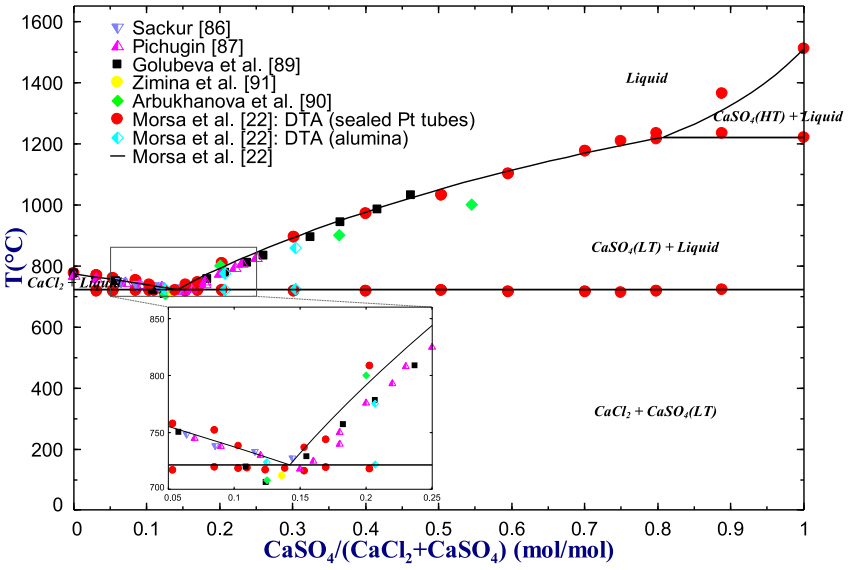

Fig. 9. Phase diagram of $CaCl_2$-$CaSO_4$ system from Morsa et al. [22] and comparison with Sackur [86], Golubeva et al. [89], Pichugin [87], Zimina et al. [91] and Arbukhanova et al. [90].

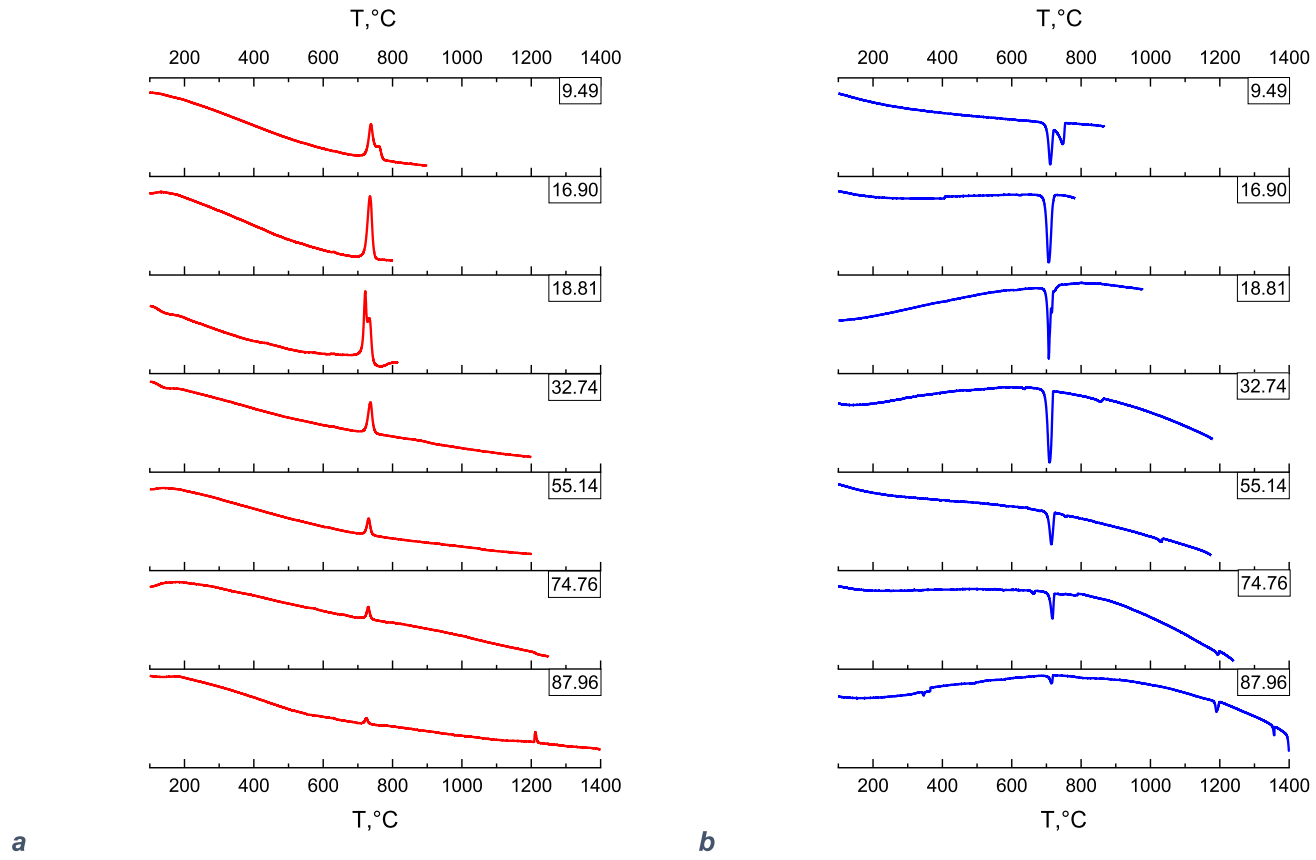

Fig. 10. DTA curves of NaCl-$CaSO_4$ mixtures, expressed in molar percentage of $CaSO_4$: a heating curves; b cooling curves.

unknown, structural modification.

4.2.2. DTA/DSC analysis

To achieve a more comprehensive understanding of the phase equilibria within the binary system, twelve mixtures (4.84, 7.93, 12.00, 14.90, 19.72, 25.00, 33.33, 39.72, 50.04, 60.12, 70.39, and 85.14 mol% $CaSO_4$) were analysed by DTA using sealed platinum tubes and results are summarised in Table S 5 and displayed in Fig. 5. The experimental results align well with previous literature [9,11–13,17,60–66] in describing the liquidus curve, as shown in Fig. 6. However, in the low-temperature range, they deviate from the experiments of [11] and instead agree with the data from [12] and [13], particularly concerning the two transitions observed at approximately 250 °C and 280 °C. These transitions also confirm those identified through HT-XRD analysis and summarised in Table 4. In reference to the DTA results, the liquidus curve reaches its maximum at a composition of 25 mol% $CaSO_4$, corresponding to the stoichiometry of $Na_6Ca(SO_4)_4$, the intermediate compound proposed by [11]. A preliminary analysis would suggest the presence of the congruently melting intermediate compound with a melting temperature of 957 °C. However, XRD analysis does not fully support this hypothesis, though it does not entirely contradict it either. In the DTA analysis within the compositional range of 15 to 70 mol% $CaSO_4$, the two low-temperature peaks were observed, with a tendency to decrease in intensity at very high sulphate concentrations. Additionally, in the heating curves for compositions of 25.0 and 33.3 mol%, another thermal event was recorded around 500 °C. Within this temperature range, a transition was observed for several compositions only in the cooling curves. The nature of this transition remains unclear; it may be attributed to the decomposition of glauberite ($Na_2Ca(SO_4)_2$) or could define the stability region of a solid solution potentially present.

To determine whether these weak effects observed in DTA are more detectable in DSC, four compositions (12.0, 25.0, 33.3, and 50.0 mol% $CaSO_4$), also analysed via XRD, were subjected to DSC measurements. These were conducted in sealed platinum tubes using platinum sample holders in a Setaram DSC. The goal was not only to assess whether the peaks were more intense and identifiable but also to estimate, through appropriate calibration, the enthalpy contents of the observed transitions, and to examine whether their compositional trend was consistent with the possible formation of an intermediate compound. Under this working hypothesis, the enthalpic contribution associated with a given transformation may be expected to be highest near the stoichiometric composition of the corresponding intermediate phase, while compositions deviating from it may show lower values. Table 6 summarises the phase transition temperatures and enthalpy values, labelled as 1 to 4, for the four analysed mixtures in DSC. The values refer to transitions observed in heating curves, which were used for the comparison of enthalpy content. It should be noted that the small enthalpic contributions associated with the low-temperature transitions labelled as “1″ and “2” are affected by relatively large uncertainties and are therefore used in the present study primarily as qualitative indicators for phase-transition identification. A more accurate determination of these low-enthalpy effects would require additional dedicated measurements. In Fig. 6, some low-temperature transitions in the mixture containing 12 mol% $CaSO_4$ and high-temperature transitions in the mixture with 50 mol% $CaSO_4$ were taken from cooling curves, as they exhibited peak splitting that was not visible in heating (see Table S 5). This peak splitting is important for describing phase stability regions within the phase diagram. The mixture with 12 mol% $CaSO_4$ exhibited a moderate enthalpy content, an order of magnitude higher than those observed in the other mixtures. Notably, the enthalpy of transition detected in the $Na_4Ca(SO_4)_3$ mixture at 562 °C is 8.22 kJ/mol.

Experimental results from DTA, DSC, and HT-XRD did not support

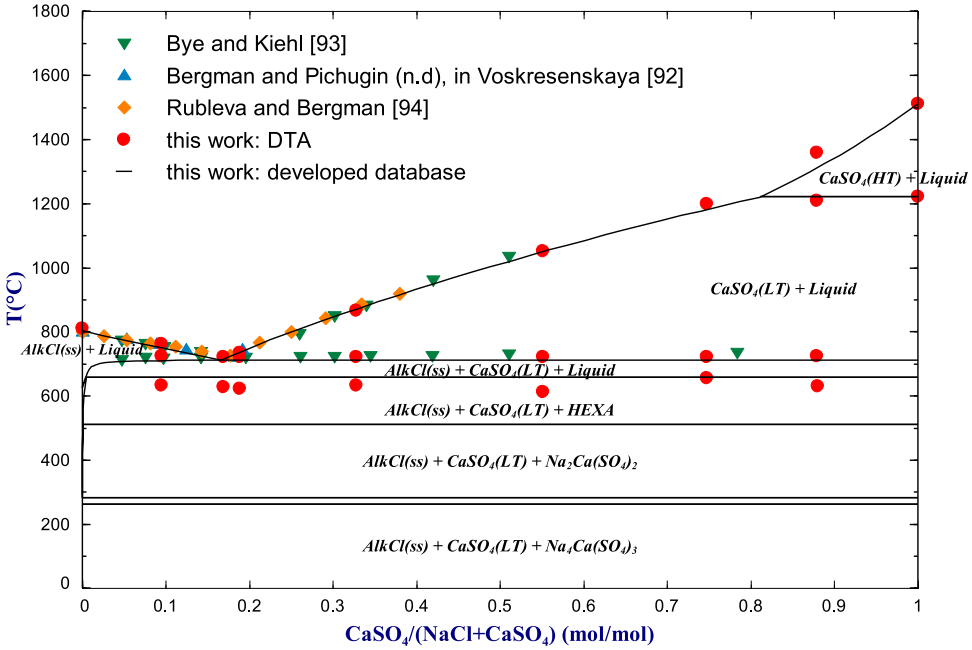

Fig. 11. Phase diagram of NaCl-$CaSO_4$ system: comparison of the developed database with experimental data from this work and Byé and Kiehl [93], Bergman and Pichugin in [92], Rubleva and Bergman [94].

the existence of the proposed intermediate compound $Na_6Ca(SO_4)_4$ [11]. This conclusion is further supported by the absence of eutectic transitions in the DTA/DSC experiments, as the presence of an intermediate compound, as proposed in the previous assessment, would have resulted in two eutectic reactions involving this intermediate compound. $Na_2Ca(SO_4)_2$ was found to be stable within a narrow temperature range, from 280 °C up to its decomposition at around 500 °C, which supports the hypothesis proposed by Freyer [60]. The transition observed at approximately 250 °C in DTA was likely associated with the decomposition of phase $Na_4Ca(SO_4)_3$. In the low-$CaSO_4$ region, the DTA results did not by themselves allow an unambiguous assignment of the observed thermal effect. However, the lack of confirmation of the intermediate compound $Na_6Ca(SO_4)_4$, and thus its exclusion from the considered phase equilibria, together with indications from previous studies [12,13,60,66], suggested the possible presence of a eutectoid reaction, which is discussed in the following section. The equilibrium line between Na_2SO_4-I solid solution and $CaSO_4$ reported in the literature was not well defined by DTA measurements, but appeared to follow a trend similar to that proposed in previous studies [12,13,60,66]. The observed splitting of certain high-temperature peaks for low $CaSO_4$--mixtures (Table S 5), mainly in cooling curves, along with supporting data from Kobertz et al. [11], suggested the possible presence of azeotropic-like points, as proposed in earlier literature [12,13,60,66]. Additionally, DTA measurements at 50 mol% $CaSO_4$ revealed peak splitting upon cooling, even more evident in DSC measurements, indicating the coexistence of eutectic and liquidus transitions. The eutectic composition appeared to be between 45 and 55 mol% $CaSO_4$. At lower concentrations, the equilibrium line defining the Na_2SO_4-I solid solution stability field, indicated by some DTA measurements (25.0 and 33.3 mol % $CaSO_4$) may have extended to higher temperatures, following the trend suggested by Speranskaya et al.'s data [13]. DTA measurements at 80–90 mol% $CaSO_4$ partially confirmed the presence of the two low-temperature transitions, as their intensity significantly decreased. However, the transition at around 500 °C was unexpectedly weak or absent during heating in the 50 mol% $CaSO_4$ mixture, despite the hypothesis that this temperature corresponded to the decomposition of that phase. Nevertheless, HT-XRD data (Fig. 4) clearly defined the stability range of this phase, supporting the proposed phase equilibria description. In the 12–33 mol% $CaSO_4$ region, the phase diagram was expected to feature four key transitions: the first, occurring at the lowest temperature, corresponded to a solid-solid transformation of pure Na_2SO_4; the second was associated with the eutectoid reaction; the third corresponded to the decomposition of $Na_4Ca(SO_4)_3$; and the fourth marked the formation of $Na_2Ca(SO_4)_2$. This interpretation, derived from experimental data, provided the basis for the proposed phase diagram.

4.2.3. *Thermodynamic assessment*

A thermodynamic reassessment of the Na_2SO_4-$CaSO_4$ binary system has been performed taking into account the new experimental findings presented above (see Sections 4.2.1 and 4.2.2). The $Na_6Ca(SO_4)_4$ compound, which was included in a previous assessment [19], based on earlier experimental findings [11], has been excluded. In contrast, the $Na_4Ca(SO_4)_3$ compound has been introduced into the thermodynamic description. Furthermore, the stability ranges of $Na_2Ca(SO_4)_2$ and $Na_4Ca(SO_4)_3$ have been redefined through the optimisation of their standard enthalpy and entropy of formation. A significant Ca solid solubility within the high-temperature modification of Na_2SO_4 (HEXA) has been introduced to the revised dataset. The optimised interaction parameters between sodium and calcium in the first sublattice of HEXA enabled an accurate description of the solid-liquid transformations across the concentration range of 0–45 mol% $CaSO_4$, including the azeotropic-like point that is characteristic of this system. The calculated phase diagram of the system Na_2SO_4-$CaSO_4$ is presented in Fig. 7, alongside the corresponding experimental data points. The reactions occurring in the system are listed in Table 7, where the values obtained in the present work are compared with the corresponding literature data.

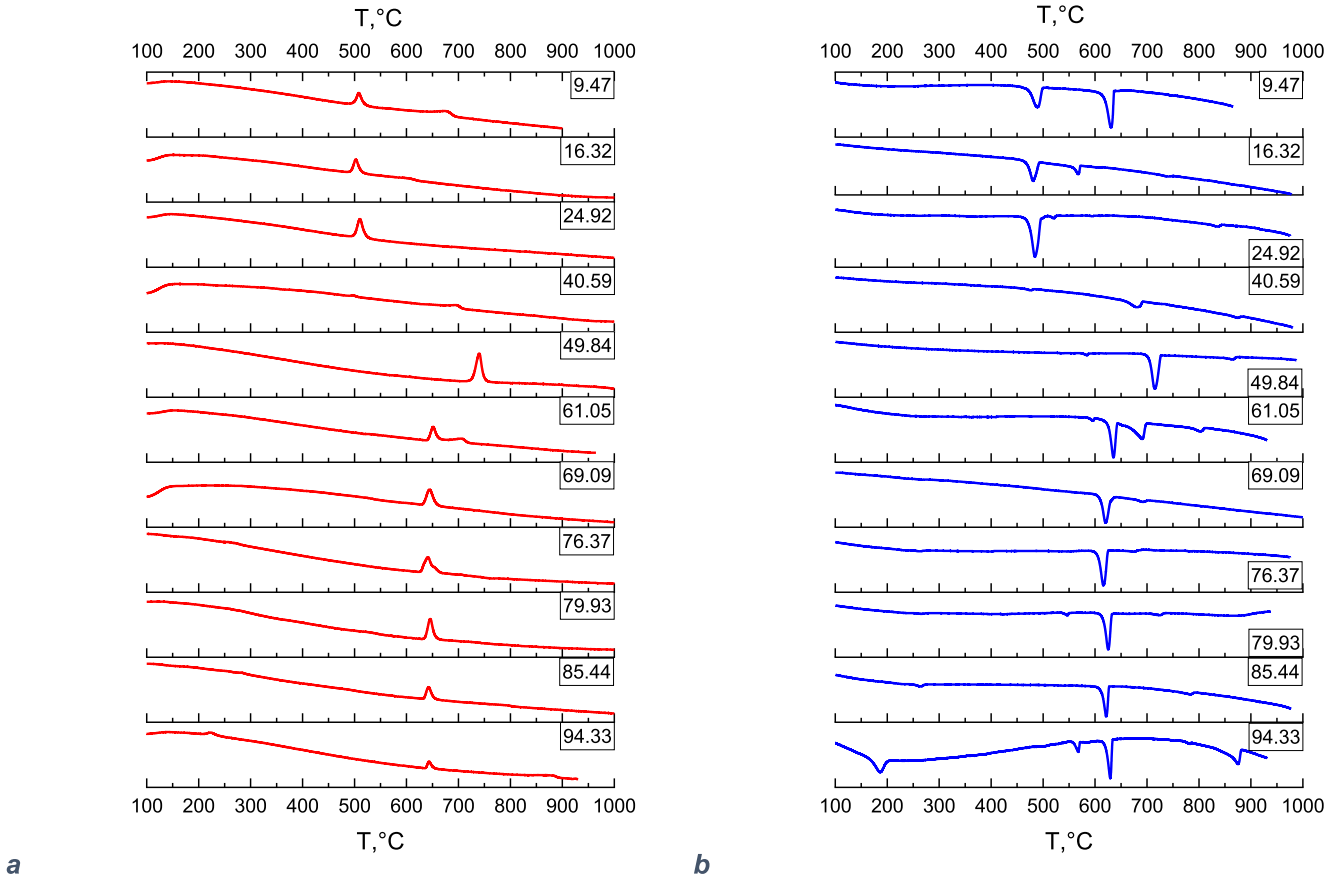

Fig. 12. DTA curves of $CaCl_2$-Na_2SO_4 mixtures, expressed in molar percentage of Na_2SO_4: a heating curves; b cooling curves.

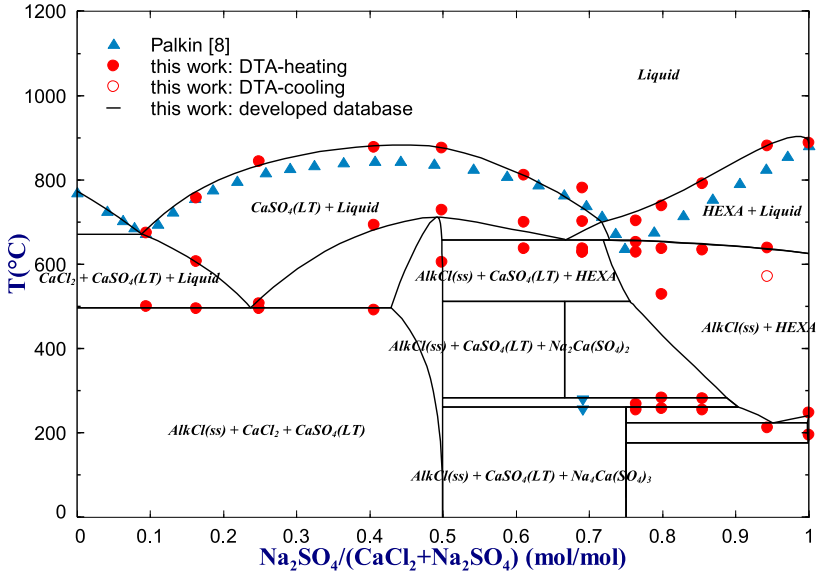

Fig. 13. Phase diagram of $CaCl_2$-Na_2SO_4 system: comparison of the developed database with experimental data from this work and Palkin [8].

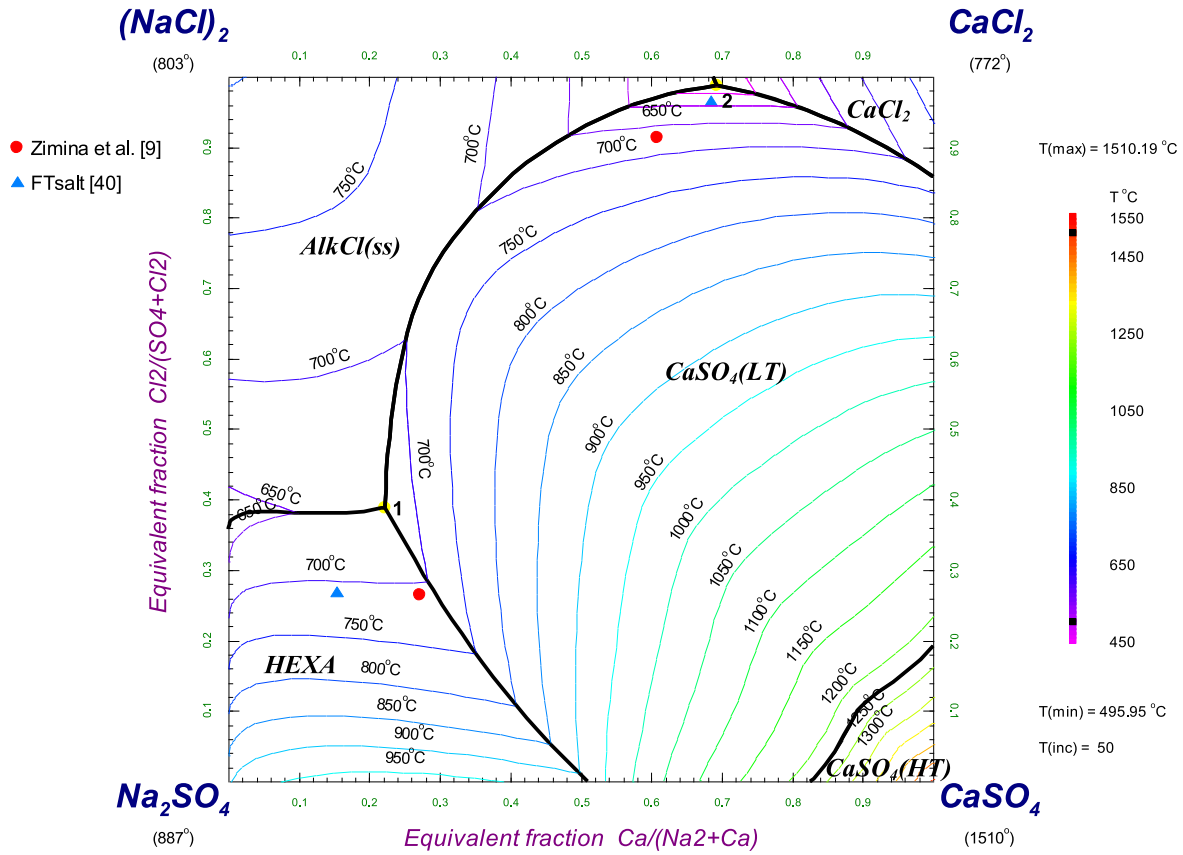

Fig. 14. Calculated liquidus surface of the reciprocal system Na^+, Ca^{2+} // Cl^-, SO_4^{2-}, and invariant points from Zimina et al. [9] and FTsalt database [40].

Table 8
Experimental and calculated invariant points, expressed in equivalent fractions, in the reciprocal system Na^+, Ca^{2+} // Cl^-, SO_4^{2-}.

	$\frac{Ca}{Na_2+Ca}$	$\frac{Cl_2}{SO_4+Cl_2}$	T, °C	Solid phase	Ref.
1	0.2229	0.3882	657.5	AlkCl(ss), HEXA, $CaSO_4$	[a]
2	0.6925	0.9877	496.0	AlkCl(ss), $CaCl_2$, $CaSO_4$	[a]
1	0.2711	0.2642	634	NaCl, $CaSO_4$, (Na,Ca)SO_4(ss)	[9] [b]
2	0.6077	0.9130	485	NaCl, $CaCl_2$, $CaSO_4$	[9] [b]
1	0.1527	0.2675	596.1	NaCl, Na_2SO_4, $CaSO_4$	[40]
2	0.6841	0.9639	470.7	NaCl, $CaCl_2$, $CaSO_4$	[40]

[a] This work.
[b] digitised data.

The optimised parameters for both solid and liquid phases, along with the assessed Gibbs energies of the double-sulphates, provide a reliable description of the phase equilibria. All parameters are summarised in Table 9. The compound $Na_4Ca(SO_4)_3$ decomposes at 261 °C and is involved in a eutectoid reaction between the solid solution phases Na-ortho-MT and HEXA at 5.2 mol% $CaSO_4$ and 223 °C. This reaction accounts for the low-temperature experimental data reported in the present study as well as in previous works [12,61]. The solubility of Ca in Na_2SO_4(MT) was calculated by introducing the solid solution Na-ortho-MT, 0.3 mol% $CaSO_4$ at the eutectoid temperature 223 °C. The eutectoid transformation involving Na_2SO_4(LT), solid solution Na-ortho-MT and the compound $Na_4Ca(SO_4)_3$ is predicted at 170 °C. The compound $Na_2Ca(SO_4)_2$ exhibits a distinct thermal stability window, with a formation temperature of 282 °C and a decomposition temperature of 507 °C. The HEXA solid solution undergoes congruent melting at a composition of 22.3 mol% $CaSO_4$, which falls well within the composition range of 20–25 mol% reported in the literature [12,13,60,66]. The calculated transition temperature and enthalpy are 970 °C and 17.0 kJ/mol, respectively, which align with DSC measurements indicating a transition temperature of 959 °C and an enthalpy of 18.8 ± 0.7 kJ/mol (see Table 6) for a comparable $CaSO_4$ concentration of 25 mol%. The eutectic reaction is predicted to occur at 50.9 mol% $CaSO_4$ and a temperature of 915 °C, in good agreement with recent literature reports [17,19]. The calculated transition enthalpy of the eutectic mixture is 16.9 kJ/mol, which compares well with the DSC-measured value of 18.9 ± 0.6 kJ/mol for a composition of 50 mol% $CaSO_4$ (see Table 6). Thus, the updated database provides an improved thermodynamic description of the investigated binary system and shows good agreement with the experimental results obtained in the present study.

4.3. NaCl-Na_2SO_4

The phase diagram NaCl-Na_2SO_4 was experimentally investigated by thermal analysis and visual-polythermal methods [69–85] and assessed [20,21]. The phase diagram was found to be a single eutectic phase diagram with no intermediate phases or solid solutions. The eutectic point was reported to be between 45 and 48 mol% Na_2SO_4 with a melting temperature in the window 624–634 °C, as summarised in Table S 6. No thermodynamic properties of the liquid phase have been reported in the literature. Lindberg et al. [20] calculated the eutectic point at 46.7 mol% Na_2SO_4 and 625.9 °C, in agreement with experimental data [77,79,80,82]. Based on the available data in literature, a thermodynamic assessment has been conducted in the present work, and the interaction parameters $L_{ij}^{(\nu)}$ in the liquid phase of the binary system NaCl-Na_2SO_4 were optimised (Table 9). The resulting phase diagram is shown in Fig. 8. The calculated eutectic point lies at 47.34 mol% Na_2SO_4

Table 9
Thermodynamic descriptions of the liquid and solid solution phases.

Gibbs energy data, J/mol	Ref.
Liquid phase	
$^{\circ}G_{NaCl} = {}^{\circ}G_{NaCl(liquid)}$	[16]
$^{\circ}G_{CaCl_2} = {}^{\circ}G_{CaCl_2(liquid)}$	[16]
$^{\circ}G_{Na_2SO_4} = {}^{\circ}G_{Na_2SO_4(liquid)}$	[19]
$^{\circ}G_{CaSO_4} = {}^{\circ}G_{CaSO_4(liquid)}$	[19]
$L^{(0)}_{NaCl,CaCl_2} = -12778.556 + 7.2596 * T$	[16]
$L^{(1)}_{NaCl,CaCl_2} = -438.047 + 1.0472 * T$	[16]
$L^{(0)}_{CaSO_4,Na_2SO_4} = -2642.9 - 1.0951 * T$	a
$L^{(1)}_{CaSO_4,Na_2SO_4} = 11282.4 - 1 * T$	a
$L^{(0)}_{NaCl,Na_2SO_4} = 3724$	a
$L^{(1)}_{NaCl,Na_2SO_4} = 2198$	a
$L^{(0)}_{CaCl_2,CaSO_4} = 35970.8 - 21.371 * T$	[22]
$L^{(1)}_{CaCl_2,CaSO_4} = -5159.39 - 1.5534 * T$	[22]
$L^{(0)}_{NaCl,CaSO_4} = 78507.2 - 65.8391 * T$	a
$L^{(1)}_{NaCl,CaSO_4} = -13531.4$	a
Solid solution phases	
HEXA: $(Na^{1+}, Ca^{2+}, Va^{0})_2(SO_4^{2-})_1$	
$^{\circ}G_{Na_2SO_4} = {}^{\circ}G^{SGPS}_{Na_2SO_{4(HT)}}$	[36]
$^{\circ}G_{Ca_2SO_4^{2+}} = 2{}^{\circ}G_{CaSO_4(HT)} - 36483.5 + 76.975 * T$	[19]
$^{\circ}G_{VaSO_4^{2-}} = 0$	[19]
$L^{(0)}_{Ca^{2+},Na^{1+}:SO_4^{2-}} = 65007.9 - 63.782 * T$	a
Na-ortho-MT: $(Na^{1+}, Ca^{2+}, Va^{0})_2(SO_4^{2-})_1$	
$^{\circ}G_{Na_2SO_4} = {}^{\circ}G^{SGPS}_{Na_2SO_{4(MT)}}$	[19]
$^{\circ}G_{Ca_2SO_4^{2+}} = 2{}^{\circ}G_{CaSO_4(LT)} + 100385.65$	[19]
$^{\circ}G_{VaSO_4^{2-}} = 0$	[19]
$L^{(0)}_{Ca^{2+},Na^{1+}:SO_4^{2-}} = 29800 - 60 * T$	a
$L^{(1)}_{Ca^{2+},Na^{1+}:SO_4^{2-}} = -8000$	a
$L^{(0)}_{Ca^{2+},Va^{0}:SO_4^{2-}} = 80 * T$	[19]
AlkCl(ss): $(Na^{1+}, Ca^{2+}, Va^{0})(Cl^{-})$	
$^{\circ}G_{NaCl} = {}^{\circ}G_{NaCl}$	[16]
$^{\circ}G_{CaCl} = {}^{\circ}G_{CaCl_2} + 39682.0427 + 5.1166 * T$	[16]
$^{\circ}G_{VaCl^{-}} = 0$	[16]
$L^{(0)}_{Ca^{2+},Va^{0}:Cl^{-}} = -41618.41682$	[16]

[a] This work.

and 624.1 °C.

4.4. $CaCl_2$-$CaSO_4$

The $CaCl_2$-$CaSO_4$ system was investigated by several authors [8,9,86–90]. Sackur [86] reported a value of 727 °C at 14.4 mol% $CaSO_4$ as the minimum of the liquidus curve involving $CaCl_2$. Pichugin [87] studied the system in the composition range 0–25 mol% of $CaSO_4$ and presented a eutectic at 718 °C and 15 mol% $CaSO_4$. Jänecke et al. [88] only reported, in the study of reciprocal system K^+, Ca^{2+} // Cl^-, SO_4^{2-}, that the eutectic is close to high $CaCl_2$ content. Golubeva et al. [89] reported a eutectic at 706 °C and 12.5 mol% $CaSO_4$. Palkin [8] and Zimina et al. [91] confirmed the same composition with a eutectic temperature of 712 °C. Arbukhanova et al. [90] considered the same eutectic composition at 708 °C in their investigation of the ternary system CaF_2-$CaCl_2$-$CaSO_4$. The existing experimental data partially cover the composition range of the phase diagram under analysis, due to the decomposition of $CaSO_4$ above 1200 °C [30,33].

A previous experimental investigation of the $CaCl_2$-$CaSO_4$ subsystem was conducted by the authors in an earlier work [22]. This study employed a combined DTA-DSC approach, with DTA measurements performed in sealed platinum tubes to enable high-temperature analysis while circumventing the issue of calcium sulphate decomposition and vaporisation of calcium chloride. This methodology allowed for the investigation of high-$CaSO_4$-content mixtures, which would otherwise be challenging to analyse in open systems. According to the previous study, the system results to be a single eutectic phase diagram, with the eutectic composition at 14.0 mol% $CaSO_4$ and a melting temperature of 722 °C. The corresponding enthalpy of fusion, determined from calorimetric measurements, was found to be 30.2 ± 0.4 kJ/mol. The optimised interaction parameters derived from this study and incorporated into the current thermodynamic database are summarised in Table 9. The calculated phase diagram is a good agreement with all experimental data (Fig. 9), the predicted enthalpy of fusion (30.1 kJ/mol at 14.2 mol% $CaSO_4$) corresponds to the measured value.

4.5. NaCl-$CaSO_4$

The stable diagonal of the reciprocal system was studied by Bergman and Pichugin as reported in [92], who presented a eutectic point of 31.7 equiv% (16.61 mol%) $CaSO_4$ at 721 °C; Byé et al. [93] reported a eutectic at 37 wt% $CaSO_4$ (20.13 mol% in NaCl-$CaSO_4$) at 725 °C; Palkin [8] and Rubleva and Bergman [94] found the eutectic to be at 30 wt% (17.45 mol% in NaCl-$CaSO_4$). Zimina et al. [9], in the frame of the complex system Ba^{2+}, Ca^{2+}, Na^+ // Cl^-, SO_4^{2-}, confirmed a eutectic temperature of 719 °C by visual-polythermal method. Rowe [10] verified the eutectic thermal effect at 725 °C. Experimental phase diagram data from literature only provided a partial coverage of the entire composition range, because of decomposition of calcium sulphate.

4.5.1. DTA analysis

A DTA investigation of the NaCl-$CaSO_4$ system was conducted using sealed platinum tubes. Seven compositions (9.49, 16.90, 18.81, 32.74, 55.14, 74.76, and 87.95 mol% $CaSO_4$) were examined. The focus was specifically on the low-to-medium $CaSO_4$ region for validation with existing data points, and on the high-$CaSO_4$ region, which has been sparsely studied in the literature due to the challenges associated with sulphate decomposition. The decision to perform the study in sealed platinum tubes effectively mitigated this issue, enabling the acquisition of entirely new data that contribute to the refinement of the phase diagram for this system. The DTA data in the composition range with high chloride content show good agreement with previously published data [92–94], confirming their reliability and reducing the need for extensive testing of other compositions. As a result, the existing literature data are validated and considered reliable. However, compared to previous studies [92–94], the DTA measurements in this work have revealed the presence of an additional thermal event at approximately 630 °C, which is consistently observed across all the investigated compositions. The DTA curves are presented in Fig. 10, while the corresponding phase transitions are summarised in Table S 7.

4.5.2. Heat capacity and enthalpy increment

The DTA analysis indicated a minimum in liquidus temperature at a composition of 16.9 mol% $CaSO_4$. To further investigate this and gather thermodynamic data, a mixture with a composition of NaCl(83.10 mol %)-$CaSO_4$(16.90 mol%)[1] was prepared by mixing the pure components in a sealed quartz ampoule, followed by heating in a furnace at 750 °C for 30 h to equilibrate and form the mixture. The resulting heat capacity curves obtained from DSC analysis using a Setaram DSC device, as determined according to the three-step ratio method described in Section 2.2.2, are displayed in Figure S 7, while the corresponding tabulated data are reported in Table S 8. The heat capacity of the liquid phase, determined experimentally, is considered constant at 138 J/mol•K. As previously suggested by the DTA measurements, an additional peak was observed at 633 °C, preceding the melting point, with an associated enthalpy of approximately 0.52 ± 0.07 kJ/mol, obtained through

[1] For all calculations the molar mass M = 71.57 g/mol of the NaCl(83.10 mol %)-$CaSO_4$(16.90 mol%) mixture was used.

integration of the C_p curves. This peak is attributed to the fusion of the sulphate-based solid solution HEXA. According to the DSC analysis, the mixture exhibits a melting temperature of 724 °C with an enthalpy of fusion of 39.3 ± 1.7 kJ/mol obtained through integration of the C_p curves.

Additionally, XRD analysis of the studied mixture was primarily conducted to investigate the possible presence of additional phases or intermediate compounds within the binary system under study. The results exclusively revealed the presence of pure chloride and sulphate phases (Figure S 8).

4.5.3. Thermodynamic assessment

In the present study, the thermodynamic assessment of the NaCl-$CaSO_4$ system was carried out by integrating new experimental data with existing literature findings [92–94]. This evaluation was based on transition temperatures defining the phase diagram and calorimetric measurements of the liquidus minimum composition obtained in this work. The revised phase diagram, calculated using the optimised dataset, is presented in Fig. 11, while the corresponding interaction parameters are summarised in Table 9. The interaction between NaCl and $CaSO_4$ was introduced to describe the properties of this diagonal of the reciprocal system.

The calculated phase diagram exhibits a minimum in liquidus temperature at 711 °C for a composition of 16.6 mol% $CaSO_4$, which is in line with the experimentally determined minimum at 724 °C with 16.9 mol% $CaSO_4$. The minimum corresponds to the reaction AlkCl(ss) + $CaSO_4$ + Liquid ⇌ Liquid. The solidus temperature, corresponding to the reaction AlkCl(ss) + $CaSO_4$ + HEXA ⇌ AlkCl(ss) + $CaSO_4$ + Liquid, is predicted to be at 657 °C which is slightly above the experimentally obtained values ranging from 613–654 °C for the varying compositions (see Fig. 11). The calculated enthalpy difference between the solidus temperature (657 °C) and the liquidus temperature (711 °C) is 35.4 kJ/mol, in good agreement with the experimental value of 39.3 kJ/mol (Figure S 9).

4.6. $CaCl_2$-Na_2SO_4

The $CaCl_2$-Na_2SO_4 system was previously investigated experimentally by Palkin [8], whose work primarily provided liquidus temperatures. The present study aims to validate the existing literature data while providing further insights into additional phase transitions through DTA analysis conducted in sealed platinum tubes. To this end, eleven compositions (9.47, 16.32, 24.92, 40.59, 49.84, 61.05, 69.09, 76.37, 79.93, 85.44, and 94.33 mol% Na_2SO_4) were systematically analysed. The DTA curves are represented in Fig. 12 and the results are summarised in Table S 9.

Consistent with the findings from the Na_2SO_4-$CaSO_4$ system (Section 4.2) two distinct transitions were experimentally detected at approximately 255 °C and 280 °C for compositions with a high Na_2SO_4 content. These transitions are attributed to decomposition temperature of $Na_4Ca(SO_4)_3$ and formation temperature of $Na_2Ca(SO_4)_2$, reinforcing the interpretation from previous analyses on Na_2SO_4-$CaSO_4$ system.

Fig. 13 presents the calculated phase diagram in comparison with the experimental transition temperatures determined in this work by DTA, as well as data from Palkin [8]. It is important to note that no additional parameters were introduced or optimised to describe the $CaCl_2$-Na_2SO_4 interactions in the liquid phase, except the interactions between NaCl-$CaSO_4$ for the stable diagonal (chapter 4.5.3). Nevertheless, excellent agreement was achieved between the experimentally determined liquidus temperatures and the predicted values. Furthermore, nearly all additional peaks observed in the DTA curves can be correlated with specific solid-solid and solid-liquid phase transitions predicted by the calculated phase diagram, with deviations in transition temperatures remaining within a narrow margin. This includes the phase transitions associated with the solid solution based on Na_2SO_4-HT (HEXA) which was not present in a previous assessment [19]. This close correspondence underscores the robustness and reliability of this thermodynamic assessment.

5. Na^+, Ca^{2+}// Cl^-, SO_4^{2-} system

Based on the assessments of the binary sub-systems (NaCl-$CaCl_2$, Na_2SO_4-$CaSO_4$, NaCl-Na_2SO_4, $CaCl_2$-$CaSO_4$) as well as the reciprocal sub-systems Na_2SO_4-$CaCl_2$ and NaCl-$CaSO_4$ presented above, the liquidus surface for the full reciprocal system Na^+, Ca^{2+} // Cl^-, SO_4^{2-} was calculated and is shown in Fig. 14.

Five fields of primary crystallisation are predicted as follows: AlkCl (ss), $CaCl_2$, HEXA, $CaSO_4$(LT) and $CaSO_4$(HT). Two characteristic four-phase invariant points involving the liquidus were identified at equivalent fractions of $Ca/(Na_2+Ca) = 0.223$ and $Cl_2/(SO_4 + Cl_2) = 0.388$, and at $Ca/(Na_2+Ca) = 0.693$ and $Cl_2/(SO_4 + Cl_2) = 0.988$, corresponding to temperatures of 658 °C and 496 °C, respectively. The corresponding reactions are AlkCl(ss) + $CaSO_4$ + HEXA ⇌ Liquid and AlkCl (ss) + $CaSO_4$ + $CaCl_2$ ⇌ Liquid, respectively. The minimum temperature of the liquidus surface is close to the one reported by Zimina et al. [9] of 485 °C. A comparison of the invariant points calculated in this work with those reported by Zimina et al. [9] and those obtained using the FTsalt database [40], based on its constituent binary subsystems, is presented in Table 8.

Within the framework of screening potential PCM candidates, among the two invariant points of the reciprocal system, the point labeled as "2″ in Table 8 satisfies the thermodynamic criteria, exhibiting a significant enthalpy change at the corresponding transition temperature. The composition, expressed in terms of independent compounds as NaCl (45.59)-$CaCl_2$(53.46)-Na_2SO_4(0.95), shows a calculated transition enthalpy of 16.9 kJ/mol at 496 °C according to the developed thermodynamic database.

6. Conclusions

This study provided a re-assessment of the reciprocal system Na^+, Ca^{2+}// Cl^-, SO_4^{2-}, integrating new experimental investigations on selected sub-systems with existing literature data. The main conclusions can be summarised as follows:

i. A revised phase diagram for the sulphate-based Na_2SO_4-$CaSO_4$ system was proposed on the basis of new experimental evidence obtained from a combined DTA, DSC, and HT-XRD investigation.
   Within this system, the intermediate compound $Na_4Ca(SO_4)_3$ was introduced in the developed thermodynamic database, while the thermodynamic properties of compound $Na_2Ca(SO_4)_2$ were reassessed, leading to a refined description of the phase equilibria.
ii. The NaCl-$CaSO_4$ and $CaCl_2$-Na_2SO_4 sub-systems were experimentally investigated by DTA, allowing a more precise definition of the phase relationships relevant to the reciprocal system.
iii. Calorimetric analysis of the NaCl-$CaSO_4$ eutectic mixture yielded a fusion enthalpy of 39.3 ± 1.7 kJ/mol and a melting temperature of 724 °C (997 K).
iv. By incorporating the newly acquired experimental results together with the evaluated thermodynamic parameters, an updated thermodynamic database was developed for the reciprocal system and its constituent sub-systems.
   The resulting dataset provides a more consistent and reliable basis for phase equilibrium modelling and supports the identification and evaluation of potential inorganic phase change materials (PCMs) for thermal energy storage applications.

Author statement

The authors have read and approved the revised manuscript and agree to its submission to the journal. This work is original and it is not

being considered for publication elsewhere.

CRediT authorship contribution statement

Amedeo Morsa: Writing – review & editing, Writing – original draft, Visualization, Validation, Software, Methodology, Investigation, Formal analysis, Data curation, Conceptualization. **Elena Yazhenskikh:** Writing – review & editing, Writing – original draft, Visualization, Validation, Supervision, Software, Methodology, Formal analysis, Data curation, Conceptualization. **Mirko Ziegner:** Writing – review & editing, Writing – original draft, Visualization, Validation, Methodology, Investigation, Formal analysis, Data curation. **Philipp Keuter:** Writing – review & editing, Writing – original draft, Visualization, Validation, Software, Resources, Methodology. **Michael Müller:** Writing – review & editing, Visualization, Validation, Supervision, Resources, Project administration, Methodology, Funding acquisition, Conceptualization. **Dmitry Sergeev:** Writing – review & editing, Visualization, Validation, Supervision, Project administration, Funding acquisition.

Declaration of competing interest

The authors declare that they have no known competing financial interests or personal relationships that could have appeared to influence the work reported in this paper.

Acknowledgements

This work was supported by the Federal Ministry for Economic Affairs and Climate Action on the basis of a decision by the German Bundestag within the project PCM-Screening 2 (FKZ 03EN6005D).

Supplementary materials

Supplementary material associated with this article can be found, in the online version, at doi:10.1016/j.tca.2026.180317.

Data availability

Data will be made available on request.

References

[1] R.-s. Ren, F.-e. Shi, X.-m. Huang, D.-h. Jiang, Application of additives to the wet flue gas desulfurization, in: 2011 International Conference on Electric Technology and Civil Engineering (ICETCE), IEEE, 2011, pp. 1037–1040.
[2] A. Anarbayev, G. Ormanova, B. Kabylbekova, N. Vysotskaya, B.K. Kucharov, Regularities of interaction of calcium chloride of distiller liquid with natural sodium sulfate, Rasayan J. Chem. 13 (4) (2020) 2173–2180.
[3] C. Pujiastuti, Y. Ngatilah, K. Sumada, S. Muljani, A chemical effectivity study on removal of Ions Seawater Mg2+, K+, Ca2+ and SO42, Adv Sci Lett 23 (12) (2017) 12252–12255.
[4] M.A.U. Rehman, Utilization of Waste Calcium Chloride (CaCl2) For the Synthesis of Useful Chemicals, US-Pakistan Center for Advanced Studies in Energy (USPCAS-E), NUST, 2014.
[5] B. Cárdenas, N. León, High temperature latent heat thermal energy storage: phase change materials, design considerations and performance enhancement techniques, Renew. Sustain. Energy Rev. 27 (2013) 724–737.
[6] A. Abhat, Low temperature latent heat thermal energy storage: heat storage materials, Sol. Energy 30 (1983) 313–332.
[7] M.M. Kenisarin, High-temperature phase change materials for thermal energy storage, Renew. Sustain. Energy Rev. 14 (3) (2010) 955–970.
[8] A. Palkin, Evolution of the diagram of state of ternary reciprocal systems in the absence of water, Izvestiya Sektora Fiziko-Khimicheskogo Analiza, Institut Obshchei i Neorganicheskoi Khimii, Akad. Nauk SSSR 17 (1949) 228–253.
[9] T.D. Zimina, A.G. Bergman, G.I. Nagornyi, The Ba, Ca, Na //Cl, SO_4 reciprocal system, Russ. J. Inorg. Chem. 10 (1965) 1167–1171.
[10] J.J. Rowe, G. Morey, C.S. Zen, The quinary reciprocal salt system Na, K, Mg, Ca/Cl, SO_4. A review of the literature with new data, in: Geological Survey Professional Paper, 741, 1972.
[11] D. Kobertz, M. Müller, Experimental Studies And *Re*-assessment of the Quasi-Binary Systems Containing the Sulfates Of Sodium, Potassium, and Calcium By Differential Thermal Analysis And X-Ray Diffraction in CALPHAD XL, CALPHAD XL, 2011.
[12] P.W.S.K. Bandaranayake, B.E. Mellander, Electrical conductivity and phase diagram of the Na_2SO_4-$CaSO_4$ system, Solid state ion. 26 (1) (1988) 33–36.
[13] E.I. Speranskaya, I.B. Barskaya, Rentgenograficheskoe i termicheskoe issledovanie splavov sistemy Na_2SO_4-$CaSO_4$, Zhur. Neorg. Khimii 6 (1961) 1392–1396, translated in Russian Jour. Inorg. Chemistry, v. 6, no. 6, p. 715-717.
[14] P. Chartrand, A.D. Pelton, Thermodynamic evaluation and optimization of the LiCl-NaCl-KCl-RbCl-CsCl-$MgCl_2$-$CaCl_2$ system using the modified quasi-chemical model, Metall. Mater. Trans. A 32A (2001) 1361–1383.
[15] H. Yin, Z. Wang, X. Lai, Y. Wang, Z. Tang, Optimum design and key thermal property of NaCl–KCl–$CaCl_2$ eutectic salt for ultra-high-temperature thermal energy storage, Sol. Energy Mater. Sol. Cells 236 (2022) 111541.
[16] B.H. Reis, Development of a Novel Thermodynamic Database For Salt Systems With Potential As Phase Change Materials, BTU Cottbus-Senftenberg, 2021.
[17] P. Coursol, A. Pelton, P. Chartrand, M. Zamalloa, The $CaSO_4$-Na_2SO_4-CaO phase diagram, Can. metall. q. 44 (4) (2005) 537–546.
[18] H. Du, Thermodynamic assessment of the K_2SO_4-Na_2SO_4-$MgSO_4$-$CaSO_4$ system, J. Ph. Equilibria 21 (2000) 6–18.
[19] E. Yazhenskikh, T. Jantzen, D. Kobertz, K. Hack, M. Müller, Critical thermodynamic evaluation of the binary sub-systems of the core sulphate system Na_2SO_4–K_2SO_4–$MgSO_4$–$CaSO_4$, Calphad 72 (2021) 102234.
[20] D. Lindberg, R. Backman, P. Chartrand, Thermodynamic evaluation and optimization of the (NaCl+ Na2SO4+ Na2CO3+ KCl+ K2SO4+ K2CO3) system, J Chem Thermodyn 39 (7) (2007) 1001–1021.
[21] X. Liu, Z. Kang, J. Zhao, S. Huang, Y. Zhang, M. He, Preparation and thermal property characterization of NaCl–Na_2CO_3–Na_2SO_4 eutectic salt mixed with carbon nanomaterials for heat storage, Sol. Energy Mater. Sol. Cells 251 (2023) 112173.
[22] A. Morsa, E. Yazhenskikh, R.D. Jacob, M. Müller, D. Sergeev, Thermodynamics of the $MgCl_2$-$MgSO_4$ and $CaCl_2$-$CaSO_4$ systems, Calphad 91 (2025) 102888.
[23] https://www.enargus.de/pub/bscw.cgi/?op=enargus.eps2&q=PCM-2&v=10&id=2029269.
[24] T.M. Besmann, K.E. Spear, Thermochemical modeling of oxide glasses, J. Am. Ceram. Soc. 85 (12) (2002) 2887–2894.
[25] E. Yazhenskikh, K. Hack, M. Müller, Critical thermodynamic evaluation of oxide systems relevant to fuel ashes and slags. Part 1: alkali oxide–silica systems, Calphad 30 (3) (2006) 270–276.
[26] A. Morsa, E. Yazhenskikh, M. Ziegner, E. Wessel, R.D. Jacob, M. Müller, D. Sergeev, Experimental study and thermodynamic assessment of the $MgSO_4$-$CaSO_4$ system, Calphad 90 (2025) 102855.
[27] D. Sergeev, E. Yazhenskikh, D. Kobertz, K. Hack, M. Müller, Phase equilibria in the reciprocal NaCl–KCl–$NaNO_3$–KNO_3 system, Calphad 51 (2015) 111–124.
[28] J. Qi, E. Yazhenskikh, M. Ziegner, X. Zhao, G. Wu, M. Müller, D. Sergeev, Experimental study and thermochemical assessment of the reciprocal system Li^+, K^+//Cl^-, CO_3^{2-}, Calphad 83 (2023) 102603.
[29] Database GTOx, GTT-Technologies, Forschungszentrum Jülich, 2010-2025, GTT-Technologies.
[30] J. Rowe, G. Morey, I. Hansen, The binary system K_2SO_4-$CaSO_4$, J. Inorg. Nucl. Chem. 27 (1965) 53–58.
[31] R. Nacken, Ueber Langbeinit und Vanthoffit (K_2SO_4. $2MgSO_4$ und $3Na_2SO_4$. $MgSO_4$), Nachr. von Ges. Wiss. Gött. Math.-Phys. Kl. 1907 (1907) 602–613.
[32] A. Ginsberg, Über die verbindungen von magnesium-und natriumsulfat, Z. anorg. Chem. 61 (1) (1909) 122–136.
[33] J. Rowe, G. Morey, C. Silber, The ternary system K_2SO_4•$MgSO_4$•$CaSO_4$, J. Inorg. Nucl. Chem. 29 (1967) 925–942.
[34] A.S.f.T. Materials, Standard Test Method For Determining Specific Heat Capacity By Differential Scanning Calorimetry, ASTM International, 2011.
[35] D. Ditmars, S. Ishihara, S. Chang, G. Bernstein, E. West, Enthalpy and heat-capacity standard reference material: synthetic sapphire (α-Al_2O_3) from 10 to 2250 K, J Res Natl Bur Stand (1934) 87 (2) (1982) 159.
[36] (v13.1), SGPS - SGTE Pure Substances database, 2019.
[37] K. Hack, The SGTE casebook: Thermodynamics At Work, Elsevier, 2008.
[38] B. Sundman, J. Ågren, A regular solution model for phases with several components and sublattices, suitable for computer applications, J. phys. chem. solids 42 (4) (1981) 297–301.
[39] B. Reis, F. Tang, P. Keuter, M. to Baben, User-friendly and robust Calphad optimizations using Calphad Optimizer in FactSage, Calphad 88 (2025) 102800.
[40] C.W. Bale, E. Bélisle, P. Chartrand, S.A. Decterov, G. Eriksson, A.E. Gheribi, K. Hack, I.H. Jung, Y.B. Kang, J. Melançon, A.D. Pelton, S. Petersen, C. Robelin, J. Sangster, P. Spencer, M.A. Van Ende, FactSage thermochemical software and databases, 2010–2016, Calphad 54 (2016) 35–53.
[41] FactSage, Facility for the analysis of Chemical thermodynamics, Version 8.3. Available from: http://www.factsage.com/.
[42] I. Barin, Thermochemical data of pure substances, ISBN-10: 3527309934 (1995).
[43] R.A. Robie, S. Russell-Robinson, B.S. Hemingway, Heat capacities and entropies from 8 to 1000 K of langbeinite ($K_2Mg_2(SO_4)_3$), anhydrite ($CaSO_4$) and of gypsum ($CaSO_4$·$2H_2O$), Thermochim Acta 139 (1989) 67–81.
[44] K. Igarashi, H. Ohtani, J. Mochinaga, Phase diagram of the system $LaCl_3$-$CaCl_2$-NaCl, Z. Naturforsch. A 42 (12) (1987) 1421–1424.
[45] O. Menge, Die binaren systeme von $MgCl_2$ und $CaCl_2$ mit den chloriden der metalle K, Na, Ag, Pb, Cu, Zn, Sn und Cd, Z. Anorg. Allg. Chem (1911).
[46] K. Nishihara, Y. Shimizu, S. Katori, An investigation of the equilibrium diagram of the CeCl, $CaCl_2$-NaCl system, J Electrochem. Soc. Jpn. 18 (1950) 179.
[47] V. Plyushchev, F. Kovalev, I. Shakhno, Reactions of alkali and alkaline earth chlorides in melts I. Ternary system of sodium, rubidium and calcium chlorides, J. Gen. Chem. Union Sov. Social. Repub. 25 (1955) 821.
[48] I.S. Morozov, Z.N. Shevtsova, L.V. Klyukina, Izuchenie diagrammy sostoyaniya sistemy $NdCl_3$-$CaCl_2$-NaCl, Zhur. Nrorg. Khim 2 (1957) 1640–1645.

[49] A. Seltveit, H. Flood, Determination of the solidus curve by a tracer technique. The system $CaCl_2$–NaCl, Acta Chem. Scand 12 (1958) 1030–1041.
[50] A.V. Nikolskii, A.M. Zakharov, V.G. Parshikov, L.G. Vodopyanova, Izv Vyssh Ucheb Zaved Tsv, Metall, Russian, 1990, pp. 89–94.
[51] F. Landsberry, R. Page, Solidification of metallic chlorides, J. Soc. Chem. Ind 39 (1920) 37–40.
[52] T. Hattori, H. Ikezawa, R. Hirano, J. Mochinaga, Phase-diagram of ternary $PrCl_3$-$CaCl_2$-NaCl system, Nippon Kagaku Kaishi (6) (1982) 952–955.
[53] Z. Qiao, A. Du, W. Mo, J. Zhi, M. Wang, C. Zheng, S. Duan, Study on the NaCl-$CaCl_2$ binary system, Rare Met. 8 (1) (1989) 9–13.
[54] M. Borovkova, A. Orekhova, K. Aleksandrov, T. Puzanova, Study of the calcium chloride-sodium chloride system, Izv. Vyss. Uchebnykh Zaved. Tsvetnaya Met. 4 (1986) 56–59.
[55] M. Tokareva, A. Bergman, S. Kayalova, Mutual system of sodium and calcium nitrates and chlorides, Zh. Neorg. Khim 3 (8) (1958) 1909–1913.
[56] K. Scholich, Ternare systeme aus kaliumchlorid, natriumchlorid und den chloriden zweiwertiger Metalle, Neues Jahrb. Mineral. Geol. Paläontol. 43 (1920) 251–262.
[57] T. Østvold, Partial Free Energies of Alkali Chlorides in Fused Mixtures With Magnesium Chloride, Munksgaard INT PUBL LTD, 35 Norre Sogade, PO BOX 2148, DK-1016 Copenhagen, 1969, p. 688. -&.
[58] P. Sem, G. Hatem, J.-P. Bros, M. Gaune-Escard, $CaCl_2$ + KCl + NaCl molten-salt mixtures. Experimental and estimated enthalpies of mixing, J. Chem. Soc. Faraday Trans. 1: Phys. Chem. Condens. Ph. 80 (2) (1984) 297–308.
[59] J. Egan, J. Bracker, Thermodynamic properties of some binary fused chloride mixtures obtained from emf measurements, J Chem Thermodyn 6 (1) (1974) 9–16.
[60] D. Freyer, W. Voigt, K. Köhnke, The phase diagram of the system Na_2SO_4-$CaSO_4$, Eur. J. Solid State Inorg. Chem. 35 (10–11) (1998) 595–606.
[61] H. Müller, Über binäre Systeme, gebildet aus den Sulfaten der Alkalien und des Calziums, Neues Jahrb. Mineral. Geol. Paläontol. 30 (1910) 1–54.
[62] S.M. Mukimov, Z.I. Filippova, Reactions in melts of Na, K, Mg, and Ca sulfates, Tr. Inst. Khim. Akad. Nauk Uzb. SSSR Inst. Khim 2 (1949) 123–132.
[63] L. Komissarova, V. Plyushchev, S. Stepina, The reaction between sodium and calcium sulfate at high temperatures: moskov, Inst. Tonkol. Khim. Tekhnol. im. MV Lomonosova Tr. (5) (1955) 3–9.
[64] A. Bellanca, L'aftitalite nel sistema ternario K_2SO_4-Na_2SO_4-$CaSO_4$, Period. mineral. 13 (1942) 21–86.
[65] F. Kracek, Melting and transformation temperatures of mineral and allied substance, Handbook of Physical Constants, Geol. Soc. Am. Spec. Pap. (36) (1942) 140–174.
[66] D. Freyer, Untersuchungen zur phasenbildung und -stabilität im system Na_2SO_4 - $CaSO_4$ - H_2O, in die fakultät für chemie und physik. PhD thesis, Technische Universität Bergakademie Freiberg, Germany, 2000.
[67] W. Eysel, H. Höfer, K. Keester, T. Hahn, Crystal chemistry and structure of Na_2SO_4 (I) and its solid solutions, Acta Crystallogr. B: Struct. Sci. 41 (1) (1985) 5–11.
[68] A.P. Shablinskii, S.K. Filatov, S.V. Krivovichev, L.P. Vergasova, S.V. Moskaleva, E. Y. Avdontseva, A.V. Knyazev, R.S. Bubnova, Dobrovolskyite, $Na_4Ca(SO_4)_3$, a new fumarolic sulfate from the Great Tolbachik fissure eruption, Kamchatka Peninsula, Russia, Miner. Mag 85 (2) (2021) 233–241.
[69] E.I. Speranskaya, Exchange decomposition without solvent: irreversible reciprocal system of sodium and magnesium chlorides and sulphates, Bull. Acad. Sci. URSS Ser. Chim 2 (1938) 463–487.
[70] E. Akopov, A. Bergman, Quaternary reciprocal systems of the chlorides and sulfates of lithium, sodium and potassium, J. Gen. Chem. USSR Engl. Transl. (1955) 1.
[71] E. Jänecke, Über das Schmelz-und erstarrungsbild des doppelt-ternären systemes (K_2· Na_2· Mg)(Cl_2· SO_4), Z. anorg. Chem. 261 (3–4) (1950) 213–225.
[72] J. Sangster, A. Pelton, Critical Coupled Evaluation of Phase Diagrams and Thermodynamic Properties of Binary and Ternary Alkali Salt systems, Phase diagrams For Ceramists, American Ceramic Society, 1987.
[73] P.I. Fedorov, K.A. Bol'shakov, The ternary reciprocal system of the chlorides and sulfates of sodium and cobalt, Russ. J. Inorg. Chem. 4 (4) (1959) 405–407.
[74] H. Flood, T. Forland, A. Nesland, Cryoscopic measurements in fused salts at elevated temperatures, Acta Chem. Scand. (Den.) Divid. Acta Chem. Scand. B 5 (1951) 1193–1198.
[75] A. Wolters, Neues Jahrb. Min. Geol Beil. Bd 30 (1911) 55–96.
[76] O. Sackur, Fused salts as solvents I, cryoscopic investigations, Z. phys. Chem 78 (1912) 550–563.
[77] A. Bergman, A. Sementsova, Troinye sistemy na parallel-to Cl, SO_4, CO_3 ik parallel-to Cl, SO_4, CO_3, Zh. Neorg. Khimii 3 (2) (1958) 383–392.
[78] A. Bergman, E. Bakumskaya, Complex-formation and double decomposition in the reciprocal system of chlorides and sulfates of sodium and cadmium, Zh. Obs. Khimii 25 (1955) 2405–2414.
[79] G. Nagornyi, T. Zimina, Nonreversible reciprocal system of sodium and barium chlorides and sulfates, Izvest. Fiz.-Khim. Nauch.-Issledovatel. Inst. Irkutsk. Univ 2 (1953) 31–40.
[80] E. Akopov, A. Bergman, Reversible-adiagonal system of sodium and potassium chlorides and sulfates, Zh. Obs. Khim 24 (1954) 1524–1532.
[81] S. Mukimov, Double decomposition in the absence of a solvent. XLVII. Property (fusion) diagrams of the ternary systems of sodium and potassium fluorides, chlorides and sulfates, Ann. sect. anal. phys.-chim. Inst. chim. gen.(USSR) 12 (1940) 19–38.
[82] M. Klochko, Double decomposition in the absence of a solvent. XXIV. Irreversible-reciprocal system: sodium chloride-lithium sulfate, Zh. Obs. Khim 3 (1933) 1026–1039.
[83] E. Akopov, A. Bergman, Fusion diagrams for the ternary system of the sulfates of lithium, sodium and potassium, Zh. Neorg. Khim 4 (1959) 1146–1152.
[84] J. Gabčová, M. Malinovský, Experimental determination and thermodynamic analysis of the phase diagrams of the systems NaCI—Na2S04 and NaCI—NaF, (1986).
[85] E. Jänecke, The reciprocal salt couples NaCl-K_2SO_4, KCl-Na_2SO_4, Z. phys. Chem 64 (1909) 343–356.
[86] O. Sackur, Geschmolzene Salze als Lösungsmittel: erwiderung an Herrn WC Bray, Z. Phys. Chem 80 (1) (1912) 254.
[87] A.M. Pichugin, Technical Encyclopedia- special communication (n.d.): 7: 192. Appears in: Schmorak J. CaCl2-CaSO4 in Handbook of Solid-Liquid Equilibria in Systems of Anhydrous Inorganic Salts (1970). Volume I: 628. Ed. N. K. Voskresenskaya. Compilers: NK Voskresenskaya, NN Evseeva, SI Berul, IP Vereshchetina. Translated from Russian.
[88] E. Jänecke, W. Mühlhäusser, Das reziproke Salzpaar (K_2-Ca)(Cl_2-SO_4), Z. anorg. allg. Chem. 228 (1936) 241–248.
[89] M.S. Golubeva, A.G. Bergman, The ternary reciprocal system of the chlorides and sulfates of potassium and calcium, Russ. Jour. Gen. Chem. 26 (1956) 249–258.
[90] P.A. Arbukhanova, Y.A. Dibirov, N.N. Verdiev, A.M. Amadziev, The CaF_2-$CaCl_2$-$CaSO_4$ system, Russ. J. Inorg. Chem. 54 (6) (2009) 980–982.
[91] T.D. Zimina, A.G. Bergaman, G.I. Nagornyi, Vzaimnaya sistema iz khloridov i sulfatov natriya. Kaltsiya i bariya, Zhur. Neorg. Khimii 10 (9) (1965) 2145–2151.
[92] N.K. Voskresenskaya, Spravochnik po plavkosti sistem iz bezvodnykh neorganicheskikh soleĭ. Tom 1. Dvoĭnye sistemy (Handbook on the fusibility of anhydrous inorganic Salt systems, Bin. Syst.) 1 (1961).
[93] J. Bye, J. Kiehl, Etude du systeme binaire sulfate de calcium-chlorure de sodium, Bull Soc Chim Fr 15 (7–8) (1948) 847–848.
[94] V. Rubleva, A. Bergman, Equilibrium diagram of the Na_2Cl_2-K_2Cl_2-$CaSO_4$ system, Zh. Obs. Khimi 26 (1956) 651–655.